Materials Today 89 (2025) 151–171

Contents lists available at ScienceDirect

Materials Today

journal homepage: www.elsevier.com/locate/mattod

Emerging acousto-mechanical metamaterials: From physics-guided design to coupling-driven performance

Zhendong Li [a,b], Xinxin Wang [a], Zhonggang Wang [a,*], Xinwei Li [c], Xiang Yu [d], Seeram Ramakrishna [b], Yang Lu [e,*], Li Cheng [d,*]

[a] School of Traffic & Transportation Engineering, Central South University, Changsha 410075 Hunan, China
[b] Department of Mechanical Engineering, National University of Singapore, Singapore 117575 Singapore
[c] Faculty of Science, Agriculture & Engineering, Newcastle University, Singapore 567739 Singapore
[d] Department of Mechanical Engineering, The Hong Kong Polytechnic University, Kowloon, Hong Kong SAR, China
[e] Department of Mechanical Engineering, The University of Hong Kong, Pokfulam, Hong Kong SAR, China

ARTICLE INFO

Keywords:
Acousto-mechanical coupling
Metamaterial design
Architected materials
Acoustic absorption
mechanical properties

ABSTRACT

The growing demand for materials that simultaneously absorb airborne sound and sustain mechanical loads has catalyzed the rise of acousto-mechanical metamaterials (AMMs)—architected systems that embed acoustic resonances within mechanically efficient architectures, enabling multifunctionality beyond the reach of conventional materials. This review provides in-depth insights into the structural and physical principles that govern acoustic absorption—the central challenge in advancing AMMs. We classify existing architectures and reveal how tailored topologies can achieve superior resonant responses and dissipative pathways. To overcome causality-governed efficiency–thickness trade-offs, we consolidate three physics-informed enhancement strategies: coherent weak resonator coupling, geometry-driven impedance tuning, and intrinsic loss engineering—offering viable paths toward optimal absorption. Critically, we elucidate the structural origins of acousto-mechanical coupling by analyzing synergistic trends and mismatches arising from parent material, unit-cell scale, and topological interdependence. We introduce a three-tier coupling framework based on geometry-sharing levels, clarifying when acoustic and mechanical functions can be decoupled and when they demand co-optimization. Finally, we outline key challenges and propose future directions in functional integration, AI-driven development, and real-world deployment. Positioned at the intersection of geometry, physics, and multifunctionality, AMMs are poised to serve as a versatile platform for next-generation engineered systems.

Introduction

Driven by rapid urbanization and intensified industrial activity, noise pollution has escalated into a pervasive global issue. Elevated environmental noise levels are now strongly associated with a range of adverse health effects—including sleep disruption, chronic stress, increased cardiovascular risk, and premature death—posing significant challenges to both public health and engineering systems [1–3]. In parallel, persistent noise exposure impairs the performance and comfort of engineering systems such as transportation, aerospace structures, and industrial environments. Over the past decade, this challenge has spurred extensive development of acoustic metamaterials targeting noise mitigation across airborne, structural, and underwater domains [4–8]. Innovations such as low-frequency absorbers [9–12], phononic metamaterials [13–15], and advanced porous composites [16–18] have demonstrated exceptional wave-dissipation capabilities. Nevertheless, these solutions inherently suffer from insufficient mechanical robustness—particularly when confronted with structural demands for compact dimensions, lightweight design, high load-bearing capacity, or impact resistance [19–23]. Such a growing multifunctional demand has catalyzed a paradigm shift in materials research, focusing on the convergence of acoustic functionality and structural performance within unified material systems. A prominent frontier lies in the development of acousto-mechanical metamaterials (AMMs)—architected systems engineered through unique designs for airborne noise mitigation (Fig. 1). The versatility of AMMs is exemplified by their broad applicability across various engineering domains. As illustrated in Fig. 2a, transportation systems represent a critical use case: noise emissions typically

* Corresponding authors.
E-mail addresses: wangzg@csu.edu.cn (Z. Wang), ylu1@hku.hk (Y. Lu), li.cheng@polyu.edu.hk (L. Cheng).

https://doi.org/10.1016/j.mattod.2025.06.029
Received 17 April 2025; Received in revised form 1 June 2025; Accepted 16 June 2025
Available online 26 June 2025

originate from structural components of vehicle bodies or train bogies, where material solutions must concurrently address passenger comfort, environmental compliance, and mechanical durability. Similarly, in aerospace applications, acoustic liners designed for noise reduction [24,25], face stringent dual requirements—minimizing weight while reliably withstanding aerodynamic loads and operational vibrations. These scenarios highlight an urgent and largely unmet engineering need: the integration of efficient sound absorption, structural integrity, and impact resilience within unified material architectures.

As a novel class of structural materials, AMMs derive their distinctive multifunctionality and tunability primarily from architectural design. Their underlying design philosophy lies in strategically exploiting the high designability of architected materials—leveraging mechanically robust frameworks while embedding locally tailored geometries to impart superior sound absorption performance (Fig. 2b). Architected materials—also known as mechanical metamaterials—have driven transformative advances in structural design through topology-driven functionalities. By tailoring geometry across multiple length scales, they achieve exceptional mechanical attributes such as high strength-to-weight ratios and superior energy absorption, while providing a versatile platform for integrating additional physical functionalities [26–34]. Among these, airborne sound absorption holds particular promise, as it critically depends on the geometry of internal air domains rather than material composition [35–40]. Hence, the most direct and physically grounded route to achieving acousto-mechanical integration [41–55], is to endow architected materials such as lattice structures with sound-absorbing capability through structural design—without compromising, and in many cases even enhancing, their mechanical performance [56–58]. Recent studies have significantly advanced this understanding by exploring specific resonance phenomena—such as tube resonance [46], slow-sound effects [56], Helmholtz resonance [59–61]—each offering tailored routes to enhance acoustic absorption. Beyond preserving the lattice structure's periodicity, integrating MPP (micro-perforated panel) into lattice architectures also offers superior acousto-mechanical multifunctionalities. Correspondingly, analytical models describing these resonances and associated acoustic impedance are now well-established, enabling precise tuning of absorption spectrum [48,57,58]. The extent of acousto-mechanical coupling in AMMs varies with structural design—some architectures support simultaneous enhancement of both properties [57–60], while others permit decoupled optimization [61,62]. Understanding and leveraging this interplay is central to attain superior multifunctionalities, as discussed in detail in this review.

Despite rapid recent progress, the development of AMMs still lacks a coherent framework that connects structural design, physical mechanisms, and multifunctional performance. In particular, few studies have examined the underlying physical limits—the causality-governed trade-off between efficiency and thickness [63,64]. As a result, strategies for mitigating anti-resonance dips or enhancing broadband absorption remain fragmented and empirical. Likewise, while design efforts have advanced from primitive to more refined architectures, there is no unified classification of design routes or structural refinement strategies. More critically, the acousto-mechanical coupling mechanisms—central to the definition of AMMs—have not been comprehensively elucidated [52,65], especially in relation to parent material choice, unit-cell scaling, and geometric interdependence.

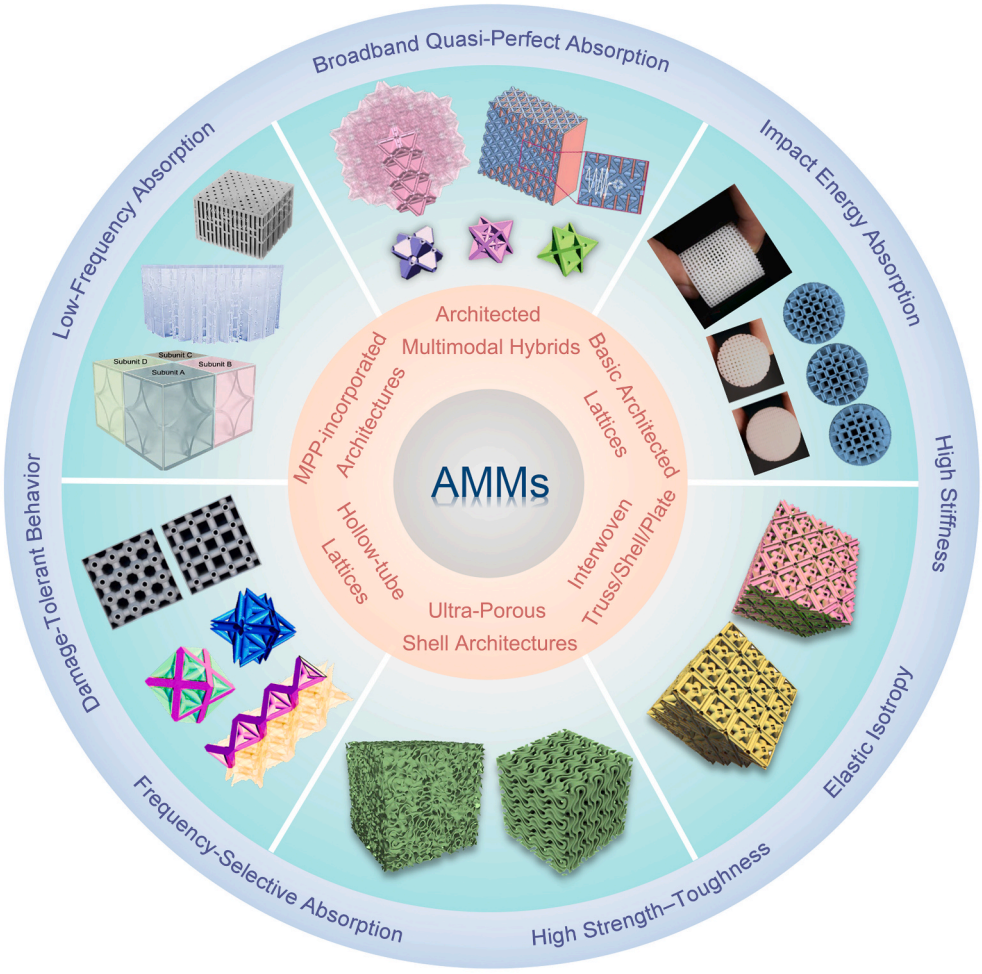

Fig. 1. Representative architectures of AMMs and their integrated functionalities. Reprinted with permission from Refs. [40,45–48,53–58].

This review bridges physics-informed design principles and functional coupling mechanisms, laying the foundation for a unified framework of AMMs. We begin by proposing a design taxonomy that overcomes geometry-induced resonance suppression—highlighting how structural interventions can enable broadband sound absorption. To move beyond empirical optimization, we examine the causality-governed trade-off between absorption efficiency and thickness, and identify three core enhancement strategies—coherent weak resonance, impedance tuning, and intrinsic loss engineering—that approach optimal absorption in compact thickness. Importantly, a coupling framework is proposed to categorize AMMs into weakly, moderately, and strongly coupled systems, based on how geometry, unit scale, and parent material collectively govern acousto-mechanical interdependence. Finally, we discuss challenges in manufacturing fidelity and absorptive dynamics under structural deformation, outline opportunities for functional expansion and AI-guided design, and position AMMs as a versatile platform for programmable multifunctionality in next-generation engineering systems.

Design principles

Architected materials have long been recognized for their mechanical efficiency, offering exceptional strength-to-weight ratio, energy dissipation, and programmable deformation. However, their potential for high-efficiency sound absorption has remained largely untapped. This gap stems from a fundamental mismatch: while mechanical performance derives primarily from solid-phase connectivity, sound absorption in air depends on the resonant behavior and viscous losses within the enclosed air domains—phenomena that must be carefully embedded into geometry [67,68]. The challenge, therefore, is not in making strong structures stronger, but in making them resonant and lossy in the right way [10,69,70].

Most architected lattice structures exhibit poor absorption due to overly connected air channels and weak confinement of acoustic energy [52,58]. To overcome this, increasingly sophisticated strategies have been proposed—not merely to modify existing geometries, but to fundamentally re-engineer how structures host resonant behavior. This section unifies these approaches under a design-centric perspective, organizing them into three archetypes: primitive, additive, and subtractive architectures. Beyond this classification, we further highlight how tailored interventions—such as embedded Helmholtz resonators, hierarchical layering, and porosity-driven dissipation—allow architected materials to transition from mechanically efficient to acoustically effective. The essence of AMM design lies in architecting topology to enable and maximize sound absorption without compromising or even enhancing mechanical properties.

Foundational architectures for acousto-mechanical metamaterials

As introduced earlier, a straightforward yet efficient approach to designing AMMs is to leverage the geometric tunability of mechanical metamaterials—modifying their topology to embed sound-absorbing

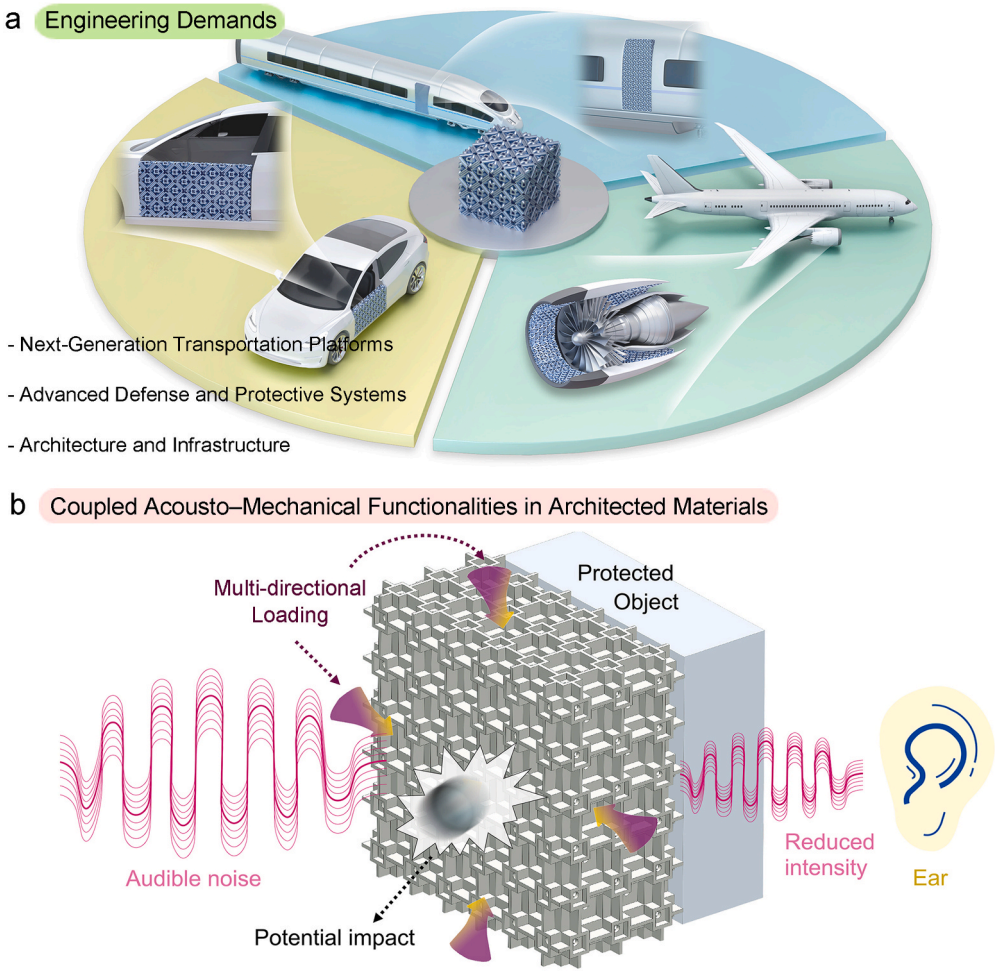

Fig. 2. Engineering demands and multifunctional mechanisms of AMMs. (a) Representative engineering scenarios highlighting the multifunctional demands. Reprinted with permission from Ref. [58]. (b) Schematic illustration of an AMM architecture simultaneously dissipating acoustic energy and resisting diverse mechanical loads. Reprinted with permission from Ref. [66].

capabilities while preserving or even enhancing mechanical properties. Accordingly, most existing AMMs are based on three-dimensional architected structures commonly found in mechanical metamaterials, including trusses, shells, plates, their hybrid or hierarchical extensions, and irregular patterns. In these systems, the unit-cell architecture—particularly its topology, spatial arrangement, and characteristic dimensions—directly governs both mechanical and acoustic responses. As illustrated in Fig. 1, representative AMM architectures—including hybrid lattices, MPP-integrated structures, hollow tubes, interwoven shell–truss systems, and ultra-porous designs—demonstrate multifunctional performance such as broadband or frequency-selective sound absorption, high stiffness, isotropic elasticity, and enhanced energy dissipation. While mechanical efficiency is often inherently supported by these architected systems, the central design challenge in AMMs lies in enabling and optimizing sound absorption. This difficulty stems from the fact that acoustic performance depends on the topology of internal air domains, which governs resonant energy dissipation via viscous and thermal mechanisms. This raises a fundamental question: What design strategies are required to achieve efficient sound absorption in mechanically robust architectures?

To address this question, we introduce a coherent classification framework that organizes existing AMM architectures into three design strategies—primitive, additive, and subtractive—each reflecting a distinct level of geometric refinement and resonance control, as shown in Fig. 3a. Primitive designs serve as the foundational configurations for most studies, while additive and subtractive strategies represent refined developments derived from these primitives—each specifically introduced to overcome the geometric and functional constraints that traditionally limit resonant acoustic responses and mechanical performance [71,72].

Primitive designs include the well-known standard lattice structures such as FCC (face-centered cubic), BCC (body-centered cubic), SC (simple cubic), and Diamond lattices, as well as TPMS (Triply Periodic Minimal Surfaces) designs like Gyroid, Schwarz-P, and Neovius. Derived from crystallographic templates and mathematical surfaces, they are typically composed of regular nodes, connecting beams, or minimal surfaces. However, these architectures—originally developed to enhance stiffness and energy absorption—feature highly connected and geometrically regular air domains that suppress the emergence of effective resonant modes, always exhibiting absorption coefficients (α) below 0.5 across relevant frequency ranges (Fig. 3b) [59,60]. As a result, their ability to dissipate acoustic energy is inherently limited. In addition, standard lattice architectures are prone to irreversible failure under compression for rigid materials—often due to low nodal or surface connectivity [53,73]. The coupled acousto-mechanical behavior of these structures, especially when implemented in materials with different elastic modulus (such as polymers versus metals), will be discussed in Section Coupling mechanisms. Overall, such limitations underscore the need for geometry-aware design strategies that simultaneously enhance structural robustness and acoustic performance.

Hence, researchers have explored additive design approaches of AMMs, which involve introducing additional structural or material elements to simultaneously enhance the acoustic absorption and mechanical properties. In Fig. 3a, additive designs are exemplified by architected hybrids, MPP-incorporated architectures, interwoven architectures, etc. These additions increase the structure's interaction with sound waves via dispersed air domain and thereby amplifying resonant effects. For example, the incorporated perforated plates can enable Helmholtz resonating effect that dissipate sound energy more effectively across targeted frequency ranges [45,61]. The interwoven strategy advances additive designs by integrating multiple primitive structures—such as truss–truss or shell–shell combinations—within a unified architectural framework [58]. The increased geometric complexity not only markedly enhances acoustic absorption through carefully designed resonator topologies, but also reinforces mechanical robustness by improving nodal connectivity and structural coherence.

Another refined design follows the subtractive concept, which, in contrast to additive approach, adopts a counterintuitive strategy of selectively removing material from the basic substrates to achieve enhanced acousto-mechanical performance. Subtractive strategies—such as strut hollowing, node volume reduction, gradient-based material removal, and topological optimization—enable the design of lightweight structures with customized acousto-mechanical properties [59,74–76]. For example, hollow struts can enhance sound absorption through a tube resonance mechanism, while simultaneously reducing the overall weight of the structure [46,54]. Subtractive designs are particularly well-suited for weight-sensitive applications such as aerospace and transportation, where mass reduction directly contributes to improved fuel efficiency and lower emissions. However, the material removal inherently alters the topology of embedded resonators and redistributes internal stress fields, introducing additional complexity to the global performance. In brief, subtractive strategies offer distinct advantages and represent a promising direction in developing AMMs.

Representative architectures and sound-absorptive behaviors

This section examines the sound-absorptive behaviors of representative AMMs across the three architectural design categories. For primitive designs, truss-based lattices, such as SC, BCC, FCC, and octet, generally offer sound absorption coefficients below 0.5 across the 1 ~ 6 kHz frequency range (i.e., relative bandwidth) [56,77], indicating inefficient dissipation of acoustic energy (Fig. 4a and Fig. 4b). Even

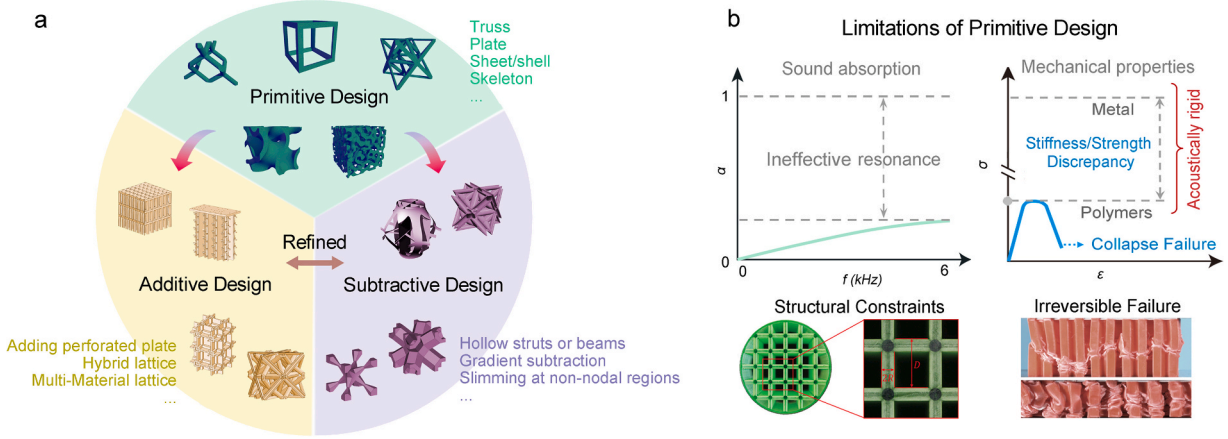

Fig. 3. Architectural design. (a) Classification of the design of AMMs—namely, primitive, additive, and subtractive design. Reprinted with permission from Refs. [48,61,74–76]. (b) Limitations of primitive design. Reprinted with permission from Refs. [59,73].

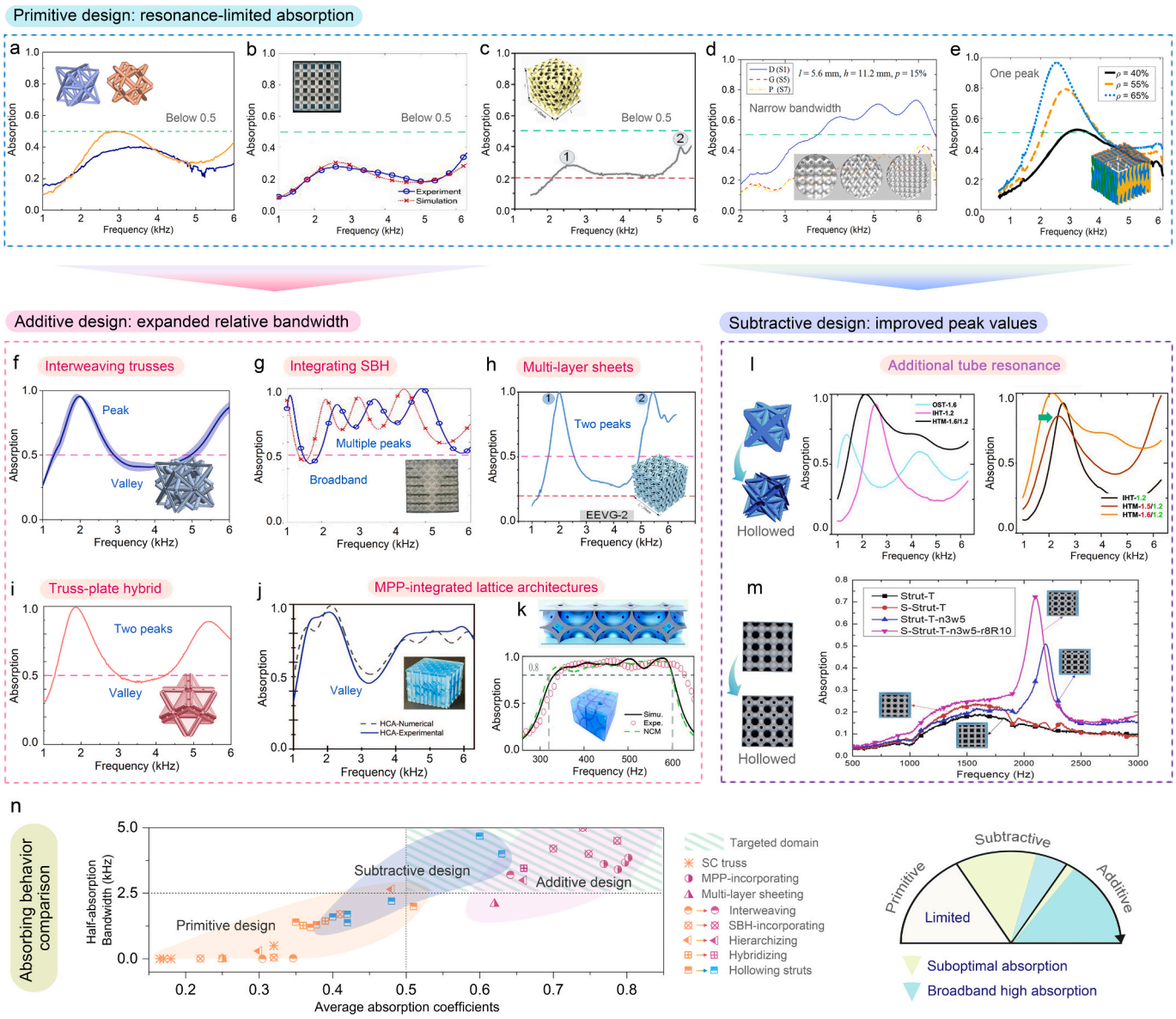

Fig. 4. Sound absorption performance of AMMs. (a)–(e) Primitive AMM architectures with limited absorption. Reprinted with permission from Refs. [55,56,60,77,85]. (f)–(k) Additive design strategies with expanded relative bandwidth. Reprinted with permission from Refs. [45,53,55–57,77]. (l)–(m) Subtractive designs with improved absorption peaks. Reprinted with permission from Refs. [46,54]. (n) Absorption comparisons of the three archetypes: Average absorption coefficients against half-absorption bandwidth (Designs: SC-truss [59], MPP-incorporating [61], multi-layer sheeting [55], interweaving [77], SBH-incorporating [56], hierarchizing [66], hybridizing [57], and hollowing struts [46]), and absorptive characteristics summarized via a pie chart.

when hollow rods are introduced, the mismatch between inner and outer diameters may lead to weak tube resonance effects [46]. TPMS structures, as shown in Fig. 4c and Fig. 4d, despite their inherently porous characteristics, exhibit limited sound attenuation across the full frequency range. This deficiency primarily arises from the excessive permeability of the structural air domain, which leads to minimal viscous losses as air flows unimpeded through the material. Physically, the predominance of open channels allows incident sound waves to propagate with limited confinement, thereby suppressing the development of oscillatory air motion and the associated energy dissipation mechanisms [78,79]. These factors constrain TPMS structures from serving as effective acoustic absorbers in practical applications. Spinodal disordered materials have also been investigated for their potential acoustic functionality owing to their interconnected, continuous air-phase morphology (Fig. 4e). Columnar variants, for example, exhibit high absorption peaks in the 2 ~ 3 kHz range—but only at high relative densities (>55 %), where the structure behaves increasingly like a solid. At such densities, the material becomes overly dense, undermining its viability for lightweight structural applications and compromising the multifunctional advantage sought in AMMs.

By leveraging well-tailored geometry–function relationships, additive designs facilitate the formation of acoustically rational air domains for efficient resonant responses, thereby widening the relative bandwidth (defined here as the half-absorption bandwidth with $\alpha \geq 0.5$). Among these, the interwoven truss strategy fully discretizes cubic air volumes into Helmholtz-like resonant chambers (see Fig. 4f). As compared to Fig. 4a, a clear absorption enhancement is observed, with absorption coefficients maintained above 0.5 across nearly the entire frequency spectrum, except for a single dip [77]. Another pioneering example is the integration of an acoustic metamaterial—specifically, a SBH (sonic black hole)—directly into truss lattices (Fig. 4g) [56]. This design achieves broadband high absorption, with an ultrahigh average coefficient of approximately around 0.8, exhibiting a substantial improvement as compared with the primitive counterparts in Fig. 4b. In

physics, the additional SBH structure induces slow sound effects, promoting energy trapping and further enhancing acoustic energy dissipation [80]. An innovative multi-layered TPMS design is illustrated in Fig. 4h [55], which significantly enhances the resonant effect and ultimately improves acoustic performance compared to the primitive design shown in Fig. 4c. Indeed, the multilayer sheet design expands the geometric design space, diversifies functional configurations, and offers greater flexibility for tailoring both acousto-mechanical properties [76]. Building upon the octet-truss, a hybrid lattice is realized by introducing micro-plates between adjacent rods (Fig. 4i) [57]. In such case, plates are introduced to form enclosed cavities, which are then perforated. With a $3 \times 3 \times 3$-unit array, the structure exhibits a dual-peak absorption profile: the first peak achieves near-perfect absorption, while the second broadens the effective frequency range—resembling the response observed in interwoven truss systems and multilayer sheet architectures. Moreover, beyond enhanced sound absorption, the integrated plate microstructures substantially improve the specific modulus and strength of the original truss by enabling membrane-like stress redistribution [41,47,81–83]. Recent advancements have also extended AMMs from periodic lattices to non-periodic, anisotropic configurations. A representative design featuring heterogeneously arranged thin walls combined with MPP is shown in Fig. 4j [53]. The MPP act as highly efficient lossy materials, similar to acoustic foams, reducing anti-resonance effects and simultaneously segmenting straight walls into varying lengths, thereby enhancing both energy dissipation and mechanical damage tolerance [61,84]. A similar strategy is seen in shell lattices integrated with MPP, as shown in Fig. 4k. By scaling up structural dimensions to target lower-frequency ranges, these designs leverage the combined effects of shell cavities and MPP-induced damping to achieve broadband low-frequency absorption—an area where conventional lattice structures often fall short.

Subtractive designs adopt a counterintuitive strategy by deliberately removing material to introduce additional energy dissipation. A representative example is the hollow-tube lattice, which employs two synergistic sound absorption mechanisms: (i) Helmholtz resonance and (ii) tube resonance [46,54]. In Fig. 4l, hollow tube lattices (abbr.: HTM) improve the absorption peaks significantly as compared to their solid counterparts. However, the effectiveness of this dual-resonance approach critically depends on a precise geometric tuning—particularly the matching effect between inner and outer diameters. Specifically, for each unit cell, the inner diameter should ideally be maximized relative to the unit size, that means, very thin struts' thickness to ensure effective tube resonance. This balance between the struts' diameters directly determines the impedance matching efficiency. Generally speaking, hollow rods in lattice structures demonstrate enhanced tube resonance [54], resulting in wider and higher absorption peaks (Fig. 4m); but unmatched geometries result in the narrow absorption bands. Subtractive designs embody the principle of "less is more", aligning perfectly with contemporary industrial goals of energy efficiency and sustainability. The reduction of material not only improves acoustic absorption but also the damage-tolerant behaviors [46]. The new mechanisms and design requirements for such strategies remain a large space to be explored.

The above discussions suggest that the refined designs—namely, additive and subtractive—can significantly enhance the absorption bandwidth and peak absorption values compared to their primitive counterparts. A more intuitive comparison of these three design paradigms is provided in Fig. 4n, where representative studies are mapped based on their average sound absorption coefficient in the $1 \sim 6$ kHz range and corresponding half-absorption bandwidth. Most data sets include comparative cases transitioning from primitive to refined designs. As shown, the figure can be divided into four quadrants. The lower-left region, indicative of poor absorption performance, is predominantly occupied by primitive designs. In contrast, subtractive designs generally shift toward the upper-right region, exhibiting clear improvements in both bandwidth and absorption coefficients. Additive designs, benefiting from greater design flexibility and the presence of more efficient architectures, are mostly clustered in the targeted broadband high-absorption domain. A conceptual pie chart is provided on the right side of the figure. This schematic qualitatively captures the performance distribution across design paradigms: primitive designs are largely constrained by limited absorption capabilities; subtractive designs, while capable of enhancing peak absorption, tend to yield a higher proportion of suboptimal cases relative to truly broadband-efficient outcomes; whereas additive designs—when judiciously engineered—demonstrate a clear dominance in high-efficiency broadband absorption, with minimal incidence of suboptimal behavior.

Design principles for desirable resonance

While both additive and subtractive designs exhibit significantly improved acoustic performance compared to primitive architectures, a unified design rationale that explains why these enhancements occur remains elusive. In this section, we move beyond geometric descriptions and explore how AMMs can be structurally refined to overcome the intrinsic limitations of weak resonance. By examining the underlying physical mechanisms, we consolidate and propose several core strategies that enable efficient sound absorption—not by coincidence, but by design.

Fig. 5a examines the internal air domain and impedance characteristics of primitive architected materials. These architectures typically contain expansive, highly-interconnected air domains, which result in low acoustic resistance and minimal energy dissipation. Functionally, they act as underdamped resonant systems, with insufficient thermal-viscous interactions to attenuate incident sound waves. Based on the underlying physical principles, we distill the advances of both additive and subtractive designs into three dominant structural refinement strategies for enhancing acoustic absorption in AMMs, as illustrated in Fig. 5b.

(1) Architecting Helmholtz resonators *in situ*: A foundational strategy for improving sound absorption in AMMs involves engineering Helmholtz resonators directly into the lattice geometry. Unlike external attachments, these *in situ* resonators are seamlessly embedded within the structural framework, creating distributed oscillation zones for air modules that drive localized viscous and thermal dissipation. When geometrically tuned to the desired frequencies, they significantly enhance sound absorption without compromising structural robustness. This approach typically encompasses two geometrically driven routes:

i) This strategy involves manipulating internal pore morphologies to form distributed Helmholtz-like cavities. Designs such as interwoven truss networks divide large air domains into discrete sub-cavities [58]; truss–plate hybrids generate enclosed pore–cavity structures [47,86]; and SBH embedded in struts introduce local resonant chambers [56]. These configurations largely enhance resonant responses, thus enabling broadband, quasi-perfect absorption.

From a theoretical perspective, these architected materials can be effectively modeled as Helmholtz resonator (HR) analogs, where the lattice geometry determines the equivalent acoustic parameters. A classical Helmholtz resonator consists of a narrow neck and a large back cavity. Its resonant frequency f_r is governed by the neck area S, neck thickness t, and cavity volume V, calculated by $f_r = c_0/2\pi\sqrt{S/(Vt)}$, where c_0 refers to sound velocity. This expression reveals how geometric parameters control the resonance condition. When extended to the MPP [87], parameters such as pore diameter d, neck thickness t, cavity depth D, and surface porosity σ collectively govern the resulting sound absorption performance. This analogy extends naturally to AMMs, where structural parameters—such as strut diameters, shell/plate thickness, and configurational patterns—directly govern the internal air domain morphology, thereby dictating equivalent HR parameters. By tailoring the structural features, designers modulate the acoustic domain geometry, altering HR-like properties to control sound absorption behavior.

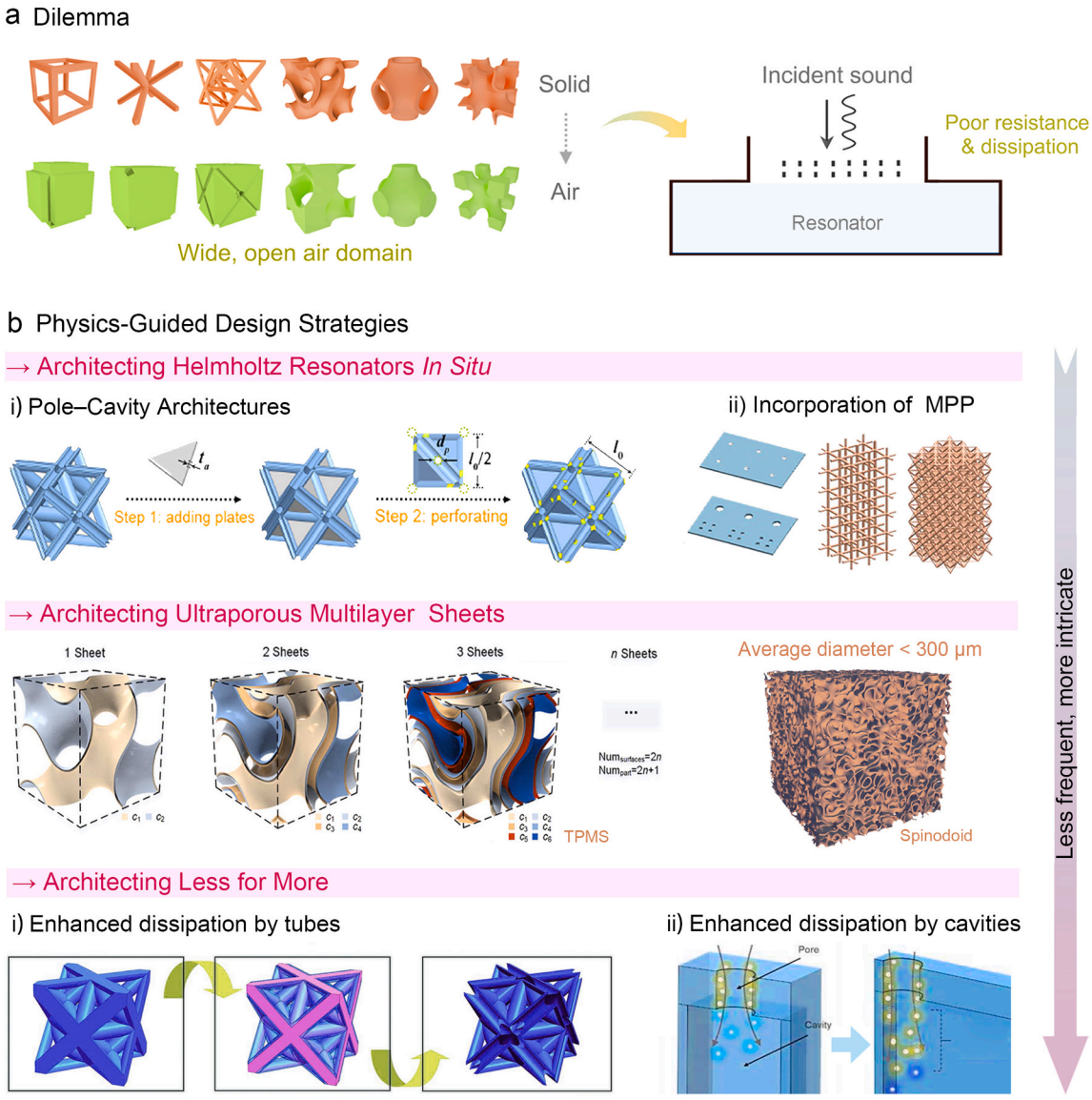

Fig. 5. Physical dilemma and strategies. (a) Primitive lattice architectures suffer from limited resonant responses due to expansive, highly connected air domains. Reprinted with permission from Ref. [58]. (b) Physics-guided design strategies to address this limitation: architecting Helmholtz resonators *in situ*, architecting ultraporous multi-layer sheets, and architecting less for more. Representative architectures for each strategy are illustrated. Reprinted with permission from Refs. [46,48,55,86,94].

This geometric-to-acoustic mapping can be achieved through direct analysis of the air domain's topology or via surrogate models that correlate structural parameters to acoustic performance. Consequently, even intricate 3D lattice architectures can be interpreted and optimized through the universal theoretical mode of MPP. For this design strategy, the impedance can be separated into contributions from the micro-perforated neck region Z_p and the cavity Z_c. The transfer matrices for the perforated layer T_p and cavity layer T_c are

$$T_p = \begin{bmatrix} 1 & Z_p \\ 0 & 1 \end{bmatrix}, T_c = \begin{bmatrix} \cos(kD) & iZ_0\sin(kD) \\ iZ_0^{-1}\sin(kD) & \cos(kD) \end{bmatrix} \tag{1}$$

where k is the wave number and Z_0 is the characteristic impedance of air. Note that in irregular Helmholtz resonators, the impedance of the perforated region Z_p includes a correction term, which are highly dependent on the specific geometry of each configuration [52,88]. These corrections capture additional viscous losses caused by boundary-layer effects near the pore edge. For an N-layer AMM, the overall matrix is the product of layer matrices in physical sequence from 1 to N:

$$T_{total} = \prod_{j=1}^{N} T_{layer}^{(j)} = \begin{bmatrix} T_{11} & T_{12} \\ T_{21} & T_{22} \end{bmatrix} \tag{2}$$

where $T_{layer}^{(j)} = T_p^{(j)} \cdot T_c^{(j)}$, representing the j-th layer transfer matrix. Then the normalized specific impedance for the cascaded units is obtained as $Z_{s,n} = Z_0^{-1} T_{11}/T_{21}$, where n means the number of parallel units. The overall normalized impedance is then obtained from its reciprocal relationship with admittance [87]. This framework enables the reduction of complex lattice-based AMM systems into tractable geometric models, allowing predictive control over their sound absorption properties through structural parameter tuning.

ii) Incorporation of MPP: Another straightforward approach is incorporating MPP into architected materials [48,61,89]. As a class of high damping material, the horizontally arranged MPP generate strong viscous and thermal boundary layer interactions with air medium by sub-millimeter perforations, providing high resistive losses without relying on soft or foam-like materials. The integration of MPPs provides

highly efficient sound attenuation across a broad frequency spectrum, particularly in the low-frequency regime. Moreover, by tuning the perforation parameters, one can readily achieve frequency tunability (see Section Structural coupling mechanisms for further details). In essence, this straightforward yet efficient strategy endows structurally robust materials with superior acoustic performance.

(2) Architecting ultraporous multi-layer sheets: A distinct strategy to enhance acoustic absorption in AMMs involves the engineering of microscale ultraporous architectures that emulate the behavior of foams (Fig. 5b). These structures promote viscous and thermal boundary-layer effects by increasing the surface-to-volume ratio and flow resistance within air pathways, thereby facilitating enhanced energy attenuation [55,76]. By layering multiple sheets, the structure creates interconnected air channels with progressively reduced cross-sectional areas and elongated lengths, forming a chain of coupled resonators. This multilevel resonance coupling broadens the absorption bandwidth, while the submillimeter pores induce strong viscous losses due to boundary-layer friction and thermal exchange—akin to the dissipation mechanisms in porous foams. The dominant mechanisms here are geometry-programmable resonance and microscale viscous damping. Structural parameters such as layer count and thickness directly tune the resonance frequencies and dissipation intensity. These designs also serve as platforms for broader multifunctional integration. Their architectural flexibility allows for graded porosity, tailored anisotropy, and hierarchical stiffness, enabling combined functionalities such as mechanical compliance, fluid regulation, and electrostatic shielding in systems where acoustic damping must be coupled with secondary roles [76]. In this context, this strategy represents a compelling approach for high-performance applications that demand both wave attenuation and structural adaptability.

Another notable example is the irregular spinodal shell architecture [90,91], which demonstrates foam-like energy dissipation behavior without relying on deterministic periodicity. When the average pore sizes below 300 μm, it behaves like the conventional porous foams. Brittany et al. [85] were among the first to utilize such architectures to realize sound absorption via the unique localized viscous drag and thermal dissipation. Owing to their inherently robust lattice framework, these structures offer promising potential for achieving superior sound absorption and mechanical properties. Although geometrically complex, these non-periodic architectures functionally resemble open-cell porous foams. By assuming a rigid-frame and relying on measured porosity, the authors performed inverse characterization to derive the transport parameters: open porosity (ϕ), airflow resistivity (σ_r), tortuosity (τ), viscous characteristic length (Λ), and thermal characteristic length (Λ'). This equivalence is justified by the similarity in dissipation mechanisms—namely, viscous and thermal losses within tortuous pore networks—which govern the behavior of both spinodoid structures and traditional acoustic foams.

(3) Architecting less for more: The third strategy targets enhanced energy dissipation by exploring mechanisms beyond Helmholtz resonance. While still in early stages, these approaches offer new avenues for improving acoustic performance through alternative or hybrid dissipation pathways (Fig. 5b). Herein, two representative directions are summarized below:

i) Tube resonance: Hollow-tube lattices introduce dual-resonance behavior by combining Helmholtz-type cavities with tube resonance [46,54]. By carefully tuning the ratio between the inner and outer diameters of tubular struts, these structures yield the tube resonating effect as the complementary pathway. Specifically, tube resonance promotes strong oscillatory airflow within the narrow channels [92], leading to intensified viscous and thermal dissipation, which works in tandem with the Helmholtz resonance occurring in the surrounding air domains.

The acoustic impedance calculation for hollow-strut cellular structures focuses on three key geometrical parameters: the inner diameter of hollow struts d_{in}, unit thickness L, and tortuosity τ — defined as the ratio of the effective acoustic path length L_e to the thickness L. The critical step involves determining L_e via the division of the strut volume by the cross-sectional area. The acoustic impedance of the hollow region can then be expressed as [92,93]:

$$Z_h = -i\frac{Z_{h0}}{\phi}\cot(k_e L_e) \tag{3}$$

where $Z_{h0} = \sqrt{\rho_e K_e}$ and $k_e = \omega\sqrt{\rho_e/K_e}$. Here, ρ_e represents the effective density while K_e represents effective bulk modulus; ω denotes the angular frequency. This expression captures the resonant behavior of the air domain confined within the hollow struts. By integrating this impedance with the contributions of the equivalent MPP components, a dual-mechanism synergy is achieved. The resulting coupled system delivers broadband sound attenuation through synergistic resonant energy trapping.

ii) Elevated cavity resonance: Another emerging approach leverages geometric tuning of the spatial relationship between the cavity wall and the entrance pores. Simulations suggest that positioning cavity walls in close proximity to the pore opening can intensify localized energy dissipation within the cavity [94]. Thus, the cavity should be shaped as a narrow rectangular prism with perforations at the ends, enabling sound waves to engage more effectively with three adjacent cavity walls. This configuration promotes stronger cavity–airflow interactions, enhancing the conversion of acoustic energy into heat. More generally, this strategy suggests that even modest geometric shift—namely, relocating pores toward cavity boundaries—can increase sound absorption. Moreover, this approach implies that, with even smaller resonance-cavity dimensions, one can achieve performance equal to or exceeding that of conventional designs. This alternative strategy does not replace but rather complement resonance-driven mechanism, expanding the design space for achieving high-performance acoustic absorption.

Strategies for optimal absorption

Design alone does not guarantee performance. Even when resonance is introduced architecturally, AMMs often suffer from large absorption dips in the mid-frequency regime—symptoms of a deeper limitation imposed by physical laws (see Fig. 4). Chief among them is the causality-governed trade-off between efficiency and thickness: a structure cannot absorb perfectly across a wide bandwidth without paying a price in spatial extent. Overcoming this constraint requires strategies informed not just by geometry, but by physics.

Despite its importance, the underlying physical mechanisms governing absorption efficiency have rarely been systematically elucidated. This section shifts the focus toward the physical constraint and provides insights into strategies for mitigating absorption dips, thereby enabling near-optimal absorption. These insights demonstrate how geometry-driven strategies—through resonant coupling, impedance tuning, and intrinsic dissipation—can be systematically orchestrated to overcome absorption dips and approach the physical limits of sound absorption in architected systems.

Causality-Governed optimal absorption

Although AMMs are defined by acousto–mechanical multifunctionality, recent advances have focused largely on sound absorption—reflecting the greater difficulty in tuning geometry-sensitive wave interactions than in achieving mechanical robustness. Broadband absorption, especially in the mid-frequency range (3 ~ 4 kHz), remains elusive due to structural impedance mismatches and underdamped resonances. This challenge is fundamentally governed by the causality principle [95,96]—a core tenet of linear acoustics that links the maximum achievable absorption to the structure's overall thickness and phase delay.

This trade-off is clearly illustrated in Fig. 6a, where the average

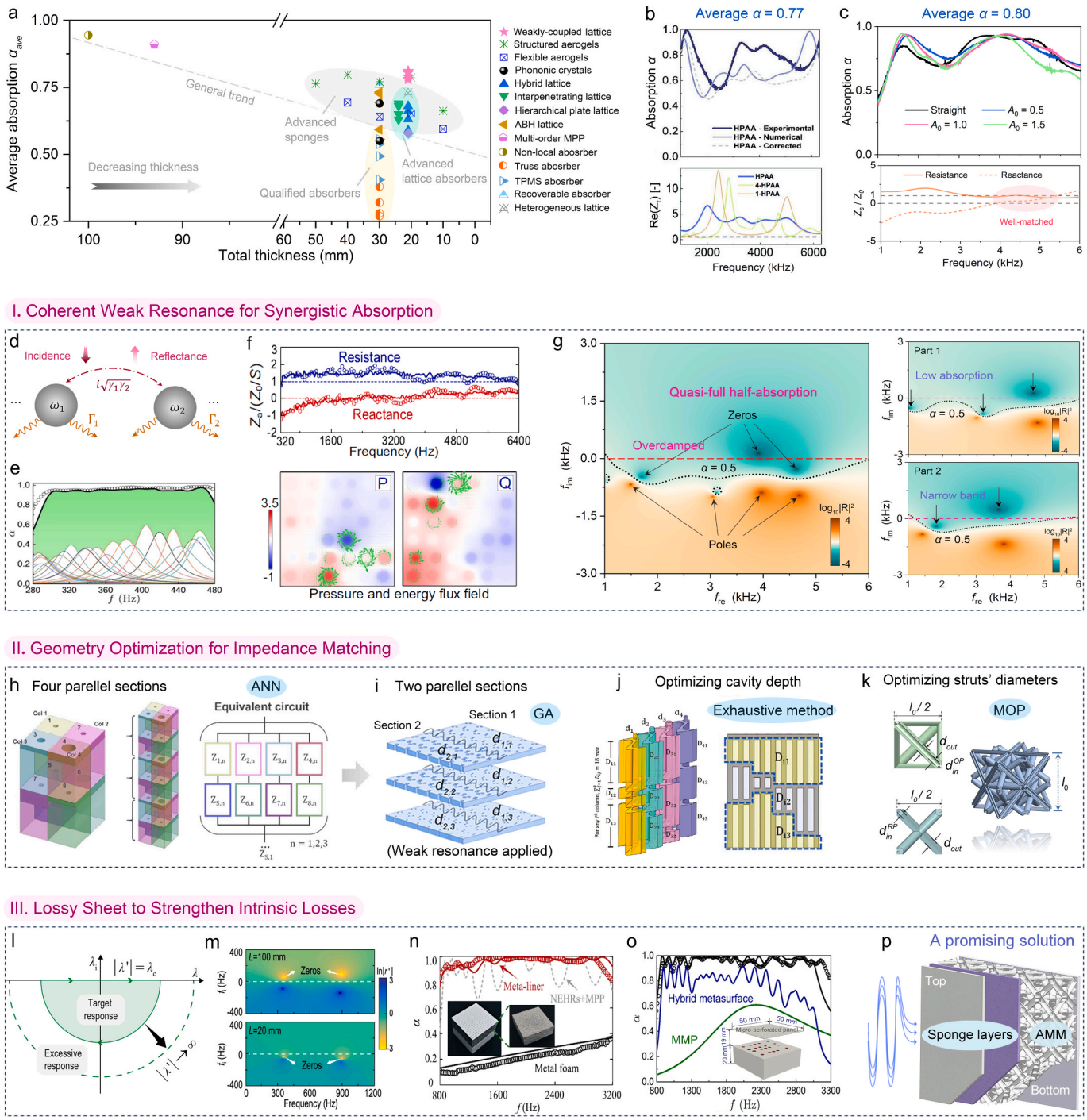

Fig. 6. Absorption efficiency and enhancement mechanisms. (a) Average sound absorption α_{ave} vs. total thickness. Superior Absorption with (b) α_{ave} = 0.77 at a thickness of 30 mm and (c) α_{ave} = 0.80 at a compact thickness of 21 mm. Reprinted with permission from Refs. [61,89]. Strategy I: (d) Coupling effect between resonant modes. (e) Enhanced absorption from modal interaction. (f) Impedance and energy flux performance under non-local coupling. (g) Reflection coefficient represented in the complex frequency plane showing desired overdamped behavior. Reprinted with permission from Refs. [61,64,99]. Strategy II: (h) Four parallel MPP sections optimized using ANN (corresponding to Fig. 6c). (i) Two parallel weak-resonator sections optimized via GA (corresponds to Fig. 6b). (j) Exhaustive optimization of cavity depth. (k) MOP-based optimization of strut diameters. Reprinted with permission from Refs. [53,58,61,89]. Strategy III: (l) Illustration of system's excessive response. (m) Reflection coefficients of two varying-length absorbers in the complex frequency plane. (n) Suppression of absorption dips by adding metal foam. (o) Absorption improvement by integrating a MPP layer. (p) Schematic of a sponge sheet affixed to the top of an AMM. Reprinted with permission from Refs. [64,97,99].

absorption coefficient α_{ave}—a key metric for acoustic performance—decreases as structural thickness is reduced [61]. In the figure, α_{ave} is calculated over the 1.0 ~ 6.0 kHz range based on reported data. Generally, thinner materials tend to exhibit inferior absorption spectra [4]. Absorbers with thicknesses around 100 mm can achieve broadband, quasi-perfect absorption [64]; however, such dimensions are impractically large for most engineering applications. While for the reported AMMs, they cluster around 30 mm thickness with α_{ave} below 0.6. Several advanced AMMs reduce the thickness to around 20 mm and approach $\alpha_{ave} \approx 0.7$. Notably, heterogeneous and weakly coupled metamaterials

achieve α_{ave} values of 0.77 by a thickness of 30 mm and 0.80 with a thickness of 21 mm [61,89], with their absorption curves shown in Fig. 6b and Fig. 6c, respectively. Noting that α_{ave} above 0.7 is considered ultrahigh [52], and achieving at 0.8 in such a compact thickness represents an unprecedented absorption efficiency among all reported AMMs. The relative impedance suggests that for the former, the normalized resistance is significantly higher than 1.0, while in the latter it oscillates closely around 1.0, indicating better impedance matching.

Building on these findings, we pose two key questions: (1) Why does this trade-off exist? (2) How can ultra-high absorption efficiency (e.g., $\alpha_{ave} \geq 0.80$) be achieved in a compact thickness?

For question 1, the answer lies in causality. The causal nature of acoustic response dictates an inequality that links the two most critical aspects of absorption: the spectral shape and the sample thickness [63]. That is, achieving near-perfect absorption in a thin material is fundamentally limited. Specifically, for a flat absorbing structure of thickness L backed by a reflective surface:

$$L \geq \frac{B_{eff}}{4\pi^2 B_0}\left|\int_0^{\infty} \ln[1-A(\lambda)]d\lambda\right| = L_{min} \tag{4}$$

where λ is the sound wavelength in air; $A(\lambda)$ is the absorption coefficient; B_{eff} denotes the effective bulk modulus and B_0 denotes the bulk modulus of air. This inequality demonstrates that the thickness quantitatively restricts the resonant response of the structure. While many advanced absorbers have approached this limit [63,64,97], breaking it is difficult without introducing additional loss (e.g., via a lossy sheet, to be discussed later).

Physics-Informed enhancement strategies

Coherently coupled weak resonance

For question 2, the emerging and promising physics-informed approaches to mitigate anti-resonance effects, broaden effective bandwidth, and approach the physical limits of absorption efficiency under compact structural constraints can be categorized as follows: (i) Coherent coupling of weak resonators, (ii) Impedance matching via geometry optimization, and (iii) Lossy-layer integration—a promising approach proposed in this review. The superiorities and mechanisms of these approaches are discussed here.

Fig. 6d-g illustrates the approach of coherent weak resonance for synergistic absorption. Coupled-mode theory offers a theoretical framework for analyzing this phenomenon [4,69,98]. According to the theory, the reflection coefficient r of a resonator in a one-port system can be expressed as:

$$r = 1 - \frac{2Q_{leak}^{-1}}{-2i(f/f_r - 1) + Q_{leak}^{-1} + Q_{loss}^{-1}} \tag{5}$$

where Q_{leak}^{-1}, Q_{loss}^{-1}, and f_r are the leakage factor, loss factor, and resonant frequency of the constituent resonator, respectively. Q_{leak}^{-1} quantifies the energy radiating out from the resonator, while Q_{loss}^{-1} characterizes the energy dissipated within the resonator. As plotted in Fig. 6d, strong coupling effect arises between multiple resonant modes. Based on Eq. (5), the absorptance can be calculated as shown below, indicating that perfect absorption ($A = 1$) is achieved under the critical-coupling condition where $Q_{leak}^{-1} = Q_{loss}^{-1}$.

$$A = \frac{4Q_{leak}^{-1}Q_{loss}^{-1}}{4(f/f_r - 1)^2 + (Q_{leak}^{-1} + Q_{loss}^{-1})^2} \tag{6}$$

For the purposes of broadband high absorption, this concept is extended by a counterintuitive scheme—coherently coupled weak resonance among individual absorbing units [99], as shown in Fig. 6e. The observed broadband absorption spectrum emerges from coherent interactions among weak resonant units. As evidenced in the absorption profiles, strategically detuned resonators create overlapping frequency bands that collectively fill attenuation troughs between individual peaks while expanding the effective bandwidth. This spectral synergy arises from enhanced mode density through multi-resonator coordination, where each unit contributes distinct yet complementary impedance characteristics. Crucially, far-field radiative coupling between elements establishes phase-matched impedance conditions that redefine wave-medium matching criteria [69]. This collective interaction mechanism enables near-perfect absorption across continuous frequency ranges in rational reactive and resistive energy conversion pathways. The synergistic interplay converts discrete narrowband peaks into a coalesced broadband response, thereby breaking the absorption bandwidth limitations, offering a promising solution for low-frequency noise mitigation [100,101].

Building on this substantial physical gain, the broadband impedance matching—key to suppressing anti-resonance, is further explored via non-local modulation (Fig. 6f) [64]. As shown, the normalized resistance slightly exceeds 1.0; meanwhile, the reactance curve oscillates around the zero axis. The significant suppression of anti-resonances, resulting from denser mode distribution, validates that this overdamped state is the most frequently observed condition in optimal sound-absorbing metamaterials. The sound pressure and energy flux fields at two specific frequencies (labeled P and Q) show that, sound energy flux clearly circulates among multiple subunits, reaching a strong non-local coupling. In compact materials, this coherent coupling mechanism can likewise be harnessed to achieve unprecedented absorption efficiency, as demonstrated in Fig. 6c. The complex frequency plane methodology can be employed to elucidate the underlying physical mechanisms (Fig. 6g) [61]. Two weak resonators—each underdamped when isolated—exhibit low absorption or narrow bandwidth. But once coupled, it transforms into an overdamped regime, confirming the critical role of dense and well-distributed resonance modes in broadband absorption.

Geometry optimization toward broadband impedance matching

The second strategy involves tuning acoustics-related structural parameters—such as pore diameter, panel thickness, and overall porosity—to modulate acoustic impedance and enhance absorption, without relying on additional resonant elements. This approach is often supported by numerical optimization tools to identify configurations with improved performance.

In one representative example (Fig. 6h), an artificial neural network (ANN) was employed to optimize pore geometries across four parallel sections [89], achieving the efficient absorption profile shown in Fig. 6b. In a subsequent study (Fig. 6i), researchers combined the weak resonance strategy with a genetic algorithm (GA), and innovatively proposed that increasing the number of smaller pores—rather than using fewer larger ones—significantly enhances absorption [61]. This design incorporated six optimized pore diameters and can be extended to more parallel or cascaded units. The resulting absorption, shown in Fig. 6c, reflects the synergistic effect of these two approaches, i.e., coherent weak resonators and structural geometry optimization, yielding unprecedented broadband absorption. Another case (Fig. 6j) explored a multilayered configuration, where unit thickness (i.e., cavity depth) was programmed in each layer [53]. The resulting heterogeneous configuration not only improved impact resilience but also retained high acoustic efficiency. In a interwoven design of truss lattice (Fig. 6k), strut diameters were optimized using a multi-objective optimization (MOP) [58]. This enabled the simultaneous enhancement of sound absorption, stiffness, and elastic isotropy—highlighting the potential of geometry-driven design even in systems with tightly linked functionalities.

In summary, optimizing acoustic parameters—particularly via AI-assisted algorithms—can guide AMMs toward favorable physical states, including broadband impedance matching and slight overdamping. Grounded in physics, this approach enables scalable and precise tuning of absorption across frequency bands while meeting mechanical demands.

Intrinsic loss engineering via lossy layers

Intrinsic loss plays a critical role in determining the acoustic energy dissipation of resonant systems. Building on recent advances in acoustic absorber theory, we propose a new physics-informed design strategy for AMMs: integrating lossy layers to enhance intrinsic damping within the architecture. To our knowledge, this approach has not yet been applied to AMMs and presents unique advantages in addressing the causality-governed trade-off between absorption efficiency and structural thickness.

As illustrated in Fig. 6l, the total response of an absorber is described in the complex plane by a function $A(\lambda)$, where λ is the complex wavelength [64]. A key insight from absorber theory is that excessive response—referring to system behavior in the asymptotic region where $\lambda \to \infty$—offers minimal contribution to actual absorption but has a disproportionately large impact on the theoretical minimum thickness L_{min}. Consequently, even small regions of inefficient damping can significantly increase the minimum required thickness of an absorber. When intrinsic losses are insufficient or poorly distributed, the system exhibits underdamped behavior, leading to flawed resonance and a degraded absorption profile. Absorbers with different lengths ($L = 100$ mm and $L = 20$ mm) both display suboptimal zero distributions—either overly sparse or located far from the real axis—indicating poor impedance matching (Fig. 6m). Importantly, these deficiencies are not rooted in geometry, but arise from intrinsic loss misallocation. This insight motivates the integration of lossy layers within AMMs to modulate damping strength and redistribute response zeros toward optimal regions. Thin, lossy coatings or embedded viscoelastic phases could be introduced into the air domain or solid skeleton to enhance absorption without introducing significant mass or volume. This design principle offers a third path for AMMs: not by introducing new resonators, but by redistributing intrinsic loss to approach the physical absorption limits under constrained geometry. Taking some examples: Ding et al. [97] proposed that adding a thin metal foam layer to stabilize relative impedance across a broadband frequency range, effectively suppressing the antiresonances (Fig. 6n), transforming the unfavorable absorption with multiple dips (gray curve) into a near-total absorption (red curve). Similarly, as shown in Fig. 6o, Huang et al. [99] proposed the concept of adding a lossy layer—MPP plate, to eliminate the absorption dips (from the blue to the black curve).

These findings highlight a critical insight: strategically introducing a lossy layer—aligned with the direction of wave propagation—offers a generalizable and physically grounded strategy for suppressing anti-resonance dips and enhancing absorption coefficient. Ultrathin layers of lossy porous materials, such as metallic foams and polymer sponges, effectively mitigates impedance mismatch at resonant frequencies, addressing the characteristic absorption minima observed in metamaterial absorbers. Crucially, the incorporation of lossy layers bridges spectral absorption gaps without compromising structural compactness, thereby approaching the minimum thickness constrained by casualty law. As illustrated in Fig. 6p, placing a thin resistive sheet atop the AMMs reshapes the distribution of response zeros without altering the primary structural geometry, thereby enhancing intrinsic damping—particularly in the mid-to-high frequency regime. When integrated with previously discussed strategies—coherently coupled resonance and structural geometry optimization—lossy-layer engineering enables AMMs to approach the efficiency–thickness bound dictated by causality. This hybrid mechanism establishes a robust pathway toward next-generation AMMs with compact dimensions and near-optimal sound absorption.

Overall, the strategies detailed in this section demonstrate how physics-driven approaches—enhanced mode density, impedance modulation, and engineered intrinsic losses—can achieve continuous, broadband absorption at mid-to-high frequencies. Yet the low-frequency regime remains an outstanding challenge: fundamental causality constraints link energy dissipation to structural size, making subwavelength broadband absorption exceedingly difficult [102]. Metamaterial solutions such as labyrinthine resonators [69,103], coiled-up channels [104,105], and membrane structures [106], represent a significant advance by achieving subwavelength absorption through localized resonances. Nevertheless, continued efforts to shrink their planar footprint—without compromising absorption performance—will be essential, rendering this compact low-frequency regime a particularly fertile ground for systematic exploration.

Coupling mechanisms

Achieving efficient sound absorption in AMMs requires the deliberate structural integration of resonant and dissipative mechanisms—a challenge that has thus far dominated the design focus. However, beyond functional coexistence, a more fundamental question arises: how are acoustic and mechanical behaviors structurally correlated within AMMs? The definition of "coupling" between acoustic absorption and mechanical properties of AMMs does not arise from direct physical interaction between wave fields, as stress and sound waves propagate through fundamentally different media—solids and air, respectively. Rather, it emerges as a function correlation, governed by shared geometric features that influence both responses. Despite its importance, this coupling has rarely been elucidated mechanistically. In this section, we elucidate how parent material stiffness, unit-cell scale, and geometric interdependence shape both sound absorption and mechanical responses—offering mechanistic insights for multifunctional design and systematic exploration of AMMs.

Parent material effect

Modern acoustic materials span a spectrum from structural composites to nano-engineered systems, each defined by its dominant energy-dissipation mechanism and mode of architectural integration. Composite materials (e.g., aerospace laminates) harness interfacial damping between layers for noise control [49,107–109]; porous media—polymer foams, mineral wool, and ceramics—provide insulation and attenuation in building and industrial exhaust systems [110]; granular fillers act as vibration dampers in machinery and mounting assemblies [111]; multifunctional nanoscale sponges and aerogels are prevailing in energy storage, thermal insulation, and flexible electronics [16–18]; and engineered metamaterials exploit subwavelength resonances for low-frequency noise-control [8]. Across this entire hierarchy—from bulky load-bearing panels down to atom-scale features—the goal remains the same: convert acoustic energy into other forms and deliver practical, reliable noise reduction in real-world applications. When the goal shifts to acousto-mechanical multifunctionality, however, material selection is driven first and foremost by stiffness—whether metals (e.g., aluminum or titanium alloys) or polymers (e.g., epoxy resin)—to satisfy load-bearing demands. This raises two central questions: (1) Do the mechanisms that govern sound absorption and structural performance work in the same way across different materials? and, if not, (2) What are the dominant operating regimes for each function, and how can we exploit their complementary strengths? With these questions in mind, the parent material effect of AMMs is discussed in this section.

The sound absorption and mechanical properties of AMMs with identical hybrid truss–plate architectures but different materials—Inconel 718 (a metallic alloy) via SLM (Selective Laser Melting), and a photopolymer resin via DLP (Digital Light Processing), are compared in Fig. 7a. It is found that the two architectures exhibit nearly identical sound absorption behavior. Specifically, the metallic AMM achieves a half-absorption bandwidth of 3.72 kHz and an average absorption coefficient of 0.65, while its polymer counterpart shows 3.86 kHz and 0.66, respectively. These minor deviations are attributed to manufacturing-induced variation rather than material-dependent acoustic response [57,86]. In contrast, mechanical properties show orders-of-magnitude differences. The metal AMM demonstrates a

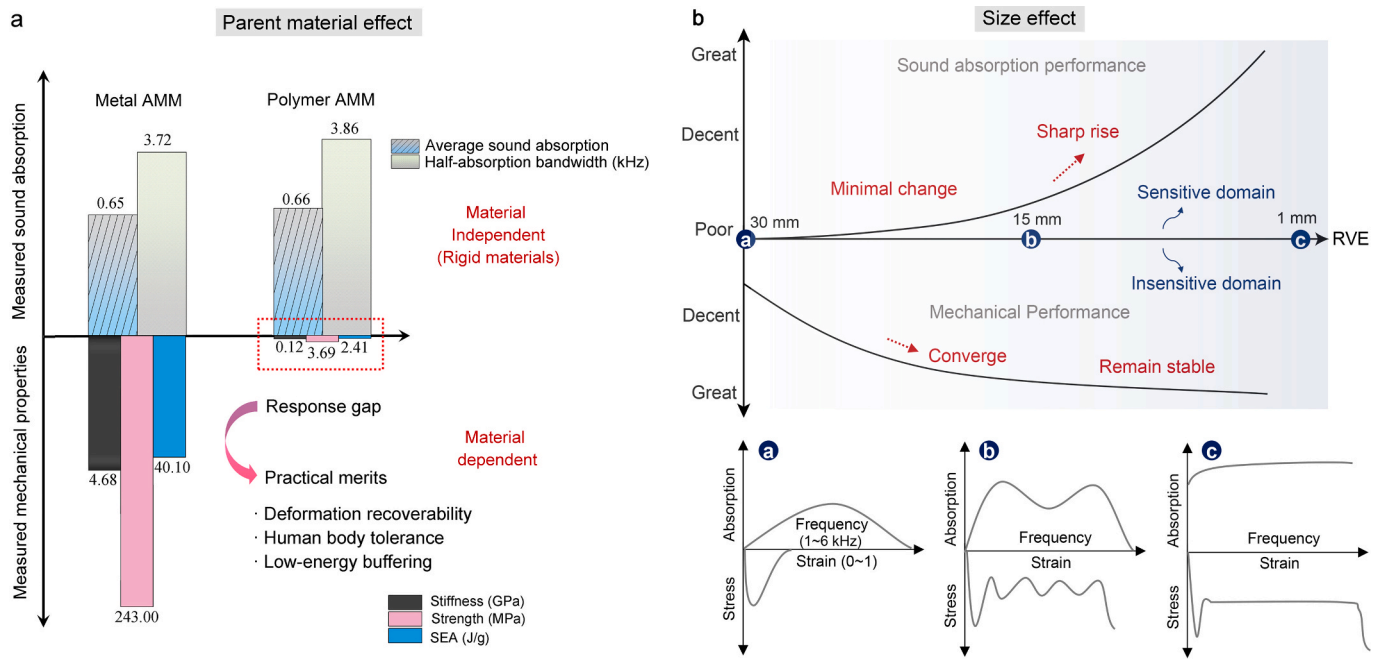

Fig. 7. Divergence in sound absorption and mechanical performance of AMMs influenced by material effect and size effect. (a) Measured acoustic and mechanical responses of identical AMM architectures fabricated using metallic and polymeric materials. (b) Size–performance mapping showing how acoustic and mechanical properties vary with RVE size. Sound absorption spectra and stress–strain curves are plotted for three representative scales, revealing their incompatible sensitivity.

stiffness of 4.68 GPa, strength of 243 MPa, and SEA (specific energy absorption) of 40.1 J/g—compared to just 0.12 GPa, 3.69 MPa, and 2.41 J/g for the polymer one. These results highlight a central principle in AMMs: unlike the material-dependent mechanical behavior, acoustic absorption is predominantly governed by structural topology.

This principle holds for rigid materials but not for elastomers of which elasticity introduces additional resonances [112,113]. By contrast, mechanical performance—particularly stiffness, strength, and energy absorption—is inherently material-dependent. Although polymers typically exhibit lower mechanical metrics than metals, this discrepancy can be leveraged as a functional advantage; that is, the large-strain deformability enables the creation of recoverable AMMs that preserve acoustic absorption even after multiple times large-strain deformation, offering pseudo-reusability [48,89]. Such resilience makes polymer-based AMMs especially well-suited for applications requiring impact mitigation and cyclic loading, including protective gear and seating systems [114]. This asymmetry between acoustic insensitivity and mechanical dependence introduces a unique design freedom: it decouples material selection from acoustic absorption, enabling geometry to be tuned for sound absorption while material choice is optimized for mechanical demand. Rather than a limitation, this material independence provides a versatile design pathway toward application-specific AMMs.

Size-dependent behaviors

In materials science, the term “size effect” traditionally refers to the phenomenon where the mechanical properties of a material vary as its characteristic dimensions—such as grain size, layer thickness, or feature scale—are reduced [115]. A classic example is the Hall–Petch relationship [116], which describes how decreasing grain size leads to increased strength due to the hindrance of dislocation motion at grain boundaries. Such effects highlight that material behavior is not governed solely by chemical composition or crystal structure, but is also strongly influenced by structure length scales. While in architected materials, size effects arise not from microstructural features but from the characteristic geometry of the architecture itself—such as unit cell size, wall thickness, and ligament length [117,118]. As a typical example, nanolattices have attracted considerable attention in recent years, demonstrating extraordinary mechanical properties across a range of studies [33,119]. Generally, the remarkable enhancement in mechanical performance is predominantly observed at the nanoscale unit cell level. But in practical engineering applications, devices and components typically fall within the millimeter to centimeter scale. To illustrate the size effect of AMMs at this practical scale, we construct a size-effect map based on the existing studies of AMMs, as shown in Fig. 7b. This map spans RVE (Representative Volume Element)—typically architectural unit cells—ranging from 1 mm to 30 mm, encompassing most reported AMMs to date (see Fig. 6a). The horizontal axis represents the RVE size. The upper half of the vertical axis represents sound absorption performance, while the lower half indicates mechanical behavior—primarily strength–toughness characteristics and energy absorption capacity as considered in this review. All data are discussed under the condition of comparable relative densities across different scales.

As shown, the size effect is particularly pronounced in shaping acoustic behavior, becoming especially evident when the RVE size increases. In the 30 ~ 15 mm range, sound absorption is generally poor, because the pore sizes of AMMs are too large to be compatible with the aperture dimensions of MPP at practical relative densities [61,99]. However, as the unit size progressively decreases from 15 mm to 1 mm, sound absorption increases sharply due to the emergence of geometrically rational resonator configurations [41,50]. When the RVE size is further reduced to the sub-millimeter scale (approximately 1 mm), the internal cavities transition into a fundamentally different acoustic regime. At this scale, the metamaterial begins to resemble an open-cell foam [59,120], where sound absorption is dominated by porous mechanisms—primarily viscous and thermal dissipation. This results in near-perfect absorption across broad frequency ranges (e.g., 0.5 to 6.0 kHz). The significant enhancement is directly attributed to the intensified interaction between incident sound waves and confined air channels. For this highly porous configuration (e.g., Spinodoid metamaterial in Fig. 5b), the wave reflections and viscosity-driven losses are amplified, further contributing to energy dissipation.

In contrast, mechanical performance exhibits a more subdued

sensitivity to scale within the same RVE range. Assuming a converged number of unit cells, a pronounced enhancement is observed as the RVE size decreases from above 30 mm. This improvement arises primarily because smaller unit dimensions help suppress global buckling and facilitate more localized load transfer. Starting from 30 mm, mechanical properties are already at a decent level; as the RVE size further decreases from 15 mm down to 1 mm, the curve generally remain stable. Hence, significant mechanical gains are generally difficult to achieve across this range [92,117,118]. Most key properties—such as stiffness, yield strength, and energy absorption—exhibit only modest, gradual increases. These marginal improvements are mainly attributed to refined fragmentation of structural members, improved stress distribution, and subtle changes in macroscopic deformation modes. In contrast to nanoscale architectures, the size-induced stiffening and defect suppression are absent at the mesoscale. Thus, mechanical enhancement across the 1 ~ 30 mm RVE range remain limited.

The scale-dependent behavior of AMMs is further elucidated via three representative cases with unit cell sizes of 30 mm, 15 mm, and 1 mm (Fig. 7b). For each case, both sound absorption (1 ~ 6 kHz) and stress–strain responses are plotted, capturing the transition in performance across scales. With RVE size of 30 mm, the sound absorption is ineffective due to limited resonance. Concurrently, the mechanical response is characterized by brittle, catastrophic failure, marked by a steep stress drop after the peak load. Such a coupled acousto-mechanical performance in both domains suggests that the structural configuration at this scale lacks features conducive to energy dissipation, either acoustically or mechanically. Reducing the RVE size to 15 mm, the coupling becomes more favorable. A broadband absorption profile with the characteristic dual-peak and single-valley curve could be achieved [53,121]. Simultaneously, the mechanical behavior transitions to a serrated stress–strain response, reflecting progressive failure and improved energy dissipation [122–125]. This alignment of enhanced damping in both domains suggests the geometry support synergistic improvements. With a 1 mm-RVE, acoustically, the structure transitions into a quasi-foam-like regime, with sub-millimeter pores enabling near-perfect broadband absorption driven by strong viscous and thermal losses [92]. Mechanically, a smooth and stable stress–strain response with high energy absorption is obtained.

In brief, size effects serve as a critical design compass for AMMs. While reducing unit size tends to improve both acoustic and mechanical performance, their sensitivities diverge across length scales—a mismatch we define as acousto-mechanical incompatibility. Acoustic absorption improves rapidly with RVE size over 15 mm, whereas mechanical properties evolve more gradually across the same size range. This mismatch creates inherent tension in simultaneous optimization, as ideal geometries for one functionality may compromise the other. Yet, understanding this trend enables rational balancing under practical manufacturing constraints—typically constrained within 1 ~ 30 mm due to the trade-off between resolution and build volume. This size effect, rooted in accumulated empirical studies and cross-validated by our synthesis—serves not only to interpret current performance limitations but to proactively guide future AMM design across scales.

Structural coupling mechanisms

Coupling strength governed by geometric interdependence

Structural geometry plays a decisive role in determining both the acoustic and mechanical responses in AMMs. Although stress waves and sound waves propagate through different physical domains—solids and air, respectively—they share a dependence on geometry for their dissipation mechanisms: elastoplastic structure deformation and viscous–thermal loss in air domain. We define the structure-level correlation between acoustic and mechanical responses as "coupling strength," reflecting the extent of geometric interdependence. Accordingly, we propose a three-tiered framework—weakly, moderately, and strongly coupled systems—as shown in Fig. 8a. Weakly coupled systems exhibit geometric separation, where distinct structural elements control either acoustic or mechanical performance independently. A representative example is MPP-incorporated architectures. As shown in Fig. 8b, sound absorption is dominated by MPP parameters such as perforation ratio, panel thickness, cavity depth, etc. Meanwhile, the underlying lattice bears most of the mechanical load [89]. This configuration enables tuning acoustic parameters without compromising mechanical integrity; but note that it increase the anisotropy as compared to periodic lattice [61]. Moderately coupled systems feature partial geometric overlap, where some design parameters affect both functions, while others can still be tuned independently. Hybrid plate–lattice systems fall into this category [47,57]. For instance, adjusting pore size or patterning on the plate modifies the resonant frequency and affects the structural rigidity to some extent. Such systems allow coordinated enhancement with

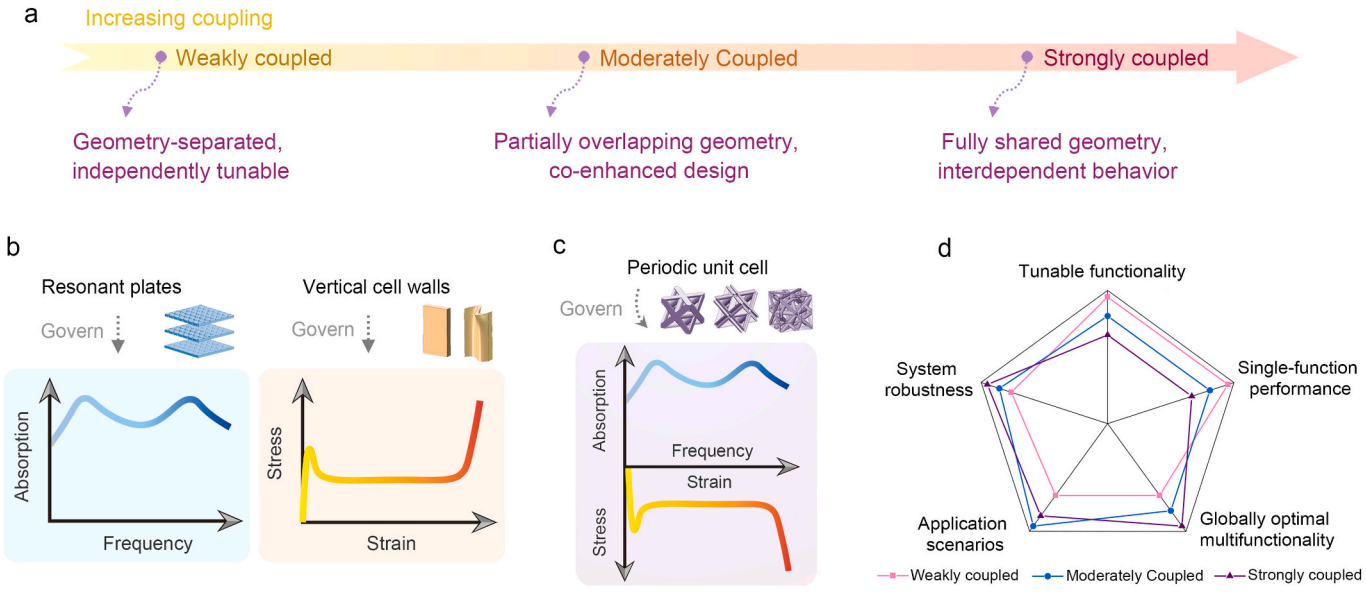

Fig. 8. Coupling strength. (a) A three-tier coupling framework based on geometry-sharing levels. Representative features of (b) a weakly coupled, and (c) strongly coupled AMM architectures. Reprinted with permission from Ref. [61]. (d) Radar chart illustrating the functional and practical characteristics across different regimes of coupling strength.

moderate synergy. Strongly coupled systems are governed by shared geometry, where the same structural features directly influence both acoustic and mechanical properties. As shown in Fig. 8c, primitive truss lattices exemplify this category. The struts' diameter, configurational pattern, and node connectivity simultaneously determine stiffness, porosity, cavity volume, and resonant behavior. Any geometric modification inherently affects both functionalities.

Note that, this classification does not assume fully decoupled or perfectly coupled extremes, as exceptions arise under specific geometric or loading conditions. For instance, even in weakly coupled systems, e.g., MPP-integrated truss lattices, extreme variations in resonant plate thickness can influence global mechanical behavior: thickened plates may alter the deformation mode, while overly thin layers may lead fail prematurely and degrade mechanical continuity. Moderately coupled systems, such as perforated plate lattices, achieve partial functional overlap through localized geometric modifications—for example, introducing pores at nodes, edges, or plate faces—which concurrently tune acoustic resonance frequencies and redistribute mechanical stress. Strongly coupled systems, typified by periodic truss/shell lattices, rely on shared geometric parameters (strut diameter, nodal spacing, and curvature) to intrinsically govern both acoustic and mechanical responses. Therefore, coupling strength should be viewed as a spectrum, sensitive to architecture and scale.

To synthesize these observations, we map the strength of acousto-mechanical coupling to key geometric features and their functional consequences, as summarized in Table 1. Weakly coupled systems exhibit minimal geometric overlap between acoustic and mechanical domains, enabled by spatially segregated components (e.g., MPP plates vs. truss cores), allowing their performance to be independently tuned. Moderately coupled systems retain partial decoupling via strategic porosity placement or hybrid plate-lattice designs. Strongly coupled systems unified geometries (e.g., periodic truss networks) to simultaneously govern both responses, thus requiring holistic, multi-objective design strategies. This three-tier coupling framework offers a rational foundation for navigating different coupling regimes and informs future directions in tailoring AMMs for application-specific multifunctionality.

Fig. 8d illustrates the functional and practical characteristics across different coupling-strength regimes. Weakly coupled architectures prioritize single-function optimization (e.g., targeted absorption frequency or mechanical strength), achieving high tunability for specific applications but limited systemic robustness. Moderately coupled designs strike a balance, enabling tunable functionality across multiple metrics while maintaining adaptable performance across diverse scenarios. Strongly coupled systems pursue globally optimal multifunctionality through integrated geometric interdependence, maximizing simultaneous acousto-mechanical efficacy at the expense of reconfigurability. The progression from weak to strong coupling reflects a fundamental design paradigm: enhanced multifunctional synergy inherently constrains component-level tunability while elevating system-wide resilience—a critical consideration when aligning architectural strategies with application-specific requirements.

Table 1
Coupling regimes in AMMs: geometric features, functional independence, and design strategies.

Coupling Strength	Geometric Overlap	Functional Independence	Research Direction	Representative architectures
Weakly Coupled	Low	High	Independent tuning for on-demand performance	MPP-integrated truss lattice
Moderately Coupled	Moderate	Moderate	Coordinated enhancement with moderate synergy	Perforated plate lattice
Strongly Coupled	High	Low	Multi-objective optimization	Truss/Shell lattice

To evaluate coupling strength quantitatively, a correlation-based approach can be applied—assuming access to sufficiently large and representative datasets. For each design instance, sound absorption and mechanical indicators can be consolidated into composite score, using entropy weighting or other multi-criteria evaluation techniques. These scores represent the overall acoustic and mechanical performance, respectively. Pearson correlation coefficient ρ can be used to evaluate the coupling strength. The coefficient $\rho \in [-1,1]$ quantifies the degree of acousto-mechanical coupling: values near $+1$ indicate strong synergy, values near 0 suggest weak or no coupling, and values approaching -1 reflect functional trade-offs. The proposed framework provides a pathway to establish measurable links between geometry and performance. Beyond linear correlations, advanced techniques—such as canonical correlation analysis or unsupervised clustering—may reveal nonlinear dependencies or hidden coupling modes, especially across different frequency or loading regimes. These data-driven methods will be essential for deciphering and optimizing multifunctionality in complex AMM architectures.

Representative architectures and multifunctional performance

In this section, we present representative weakly coupled and strongly coupled AMMs, delving into their multifunctional performance to reveal how geometric configurations and energy coupling mechanisms dictate acousto-mechanical behaviors. Weakly coupled designs effectively separate the structural units responsible for acoustic and mechanical performance, providing distinct benefits in achieving multifunctionality. Weakly coupled systems separate acoustic and mechanical domains, enabling independent tuning via modular design—e.g., MPP for absorption and NPR lattices for structural resilience (Fig. 9a) [48]. Fig. 9b shows that when equipped with varied geometric parameters of resonant panels, AMMs exhibit tunable absorption characteristics, achieving both single-frequency tuning from extremely-low to low frequencies, and broadband absorption across different spectral regimes. Concurrently, the mechanical unit's variation, including re-entrant, double-arrowhead, and SC-based, enables structural strength control, facilitating programmable large-strain deformation responses. As previously discussed in Fig. 7a, the polymer-based AMM with strengths programmed within 1 MPa (Fig. 9c), making them suitable for applications involving human-body interactions, such as protective and wearable devices.

Multi-layer MPP give rise to cascaded resonances. In Fig. 9d, a heterogeneous configuration is introduced, where each layer features distinct cavity depths, forming a serial arrangement that results in broadband absorption with high peak coefficients [53]. Mechanically, lattice units with varying depths work in concert to enhance damage resistance through strong interlayer interactions during collapse, yielding the stable stress–strain responses. However, the cavity depth is not the critical factor which affects sound absorption, and the hybrid resonance modes—arising from the combination of cascaded and parallel resonators—have not been fully exploited to maximize absorption performance. To address this, Li et al. [48] proposed an optimization strategy based on a genetic algorithm, where perforation diameters in three-layer resonant panels were constrained between 0.2 mm and 0.8 mm. The objective was to maximize the bandwidth over which the absorption coefficient exceeds 0.75. As shown in Fig. 9e, this approach yields ultrabroadband, quasi-perfect absorption with no pronounced valleys—a performance level rarely achieved in architected materials. Interestingly, the applied curved cell walls, while having negligible influence on acoustic performance, fundamentally transforms the mechanical behavior—from brittle, catastrophic collapse in straight-walled lattices to progressive, stable deformation—leading to enhanced damage tolerance, thereby forming a long and plain stress plateau (the red curve). These examples underscore the versatility of weakly coupled systems, which allow resonant plate geometries to be independently optimized for acoustic performance, while the underlying lattice can be

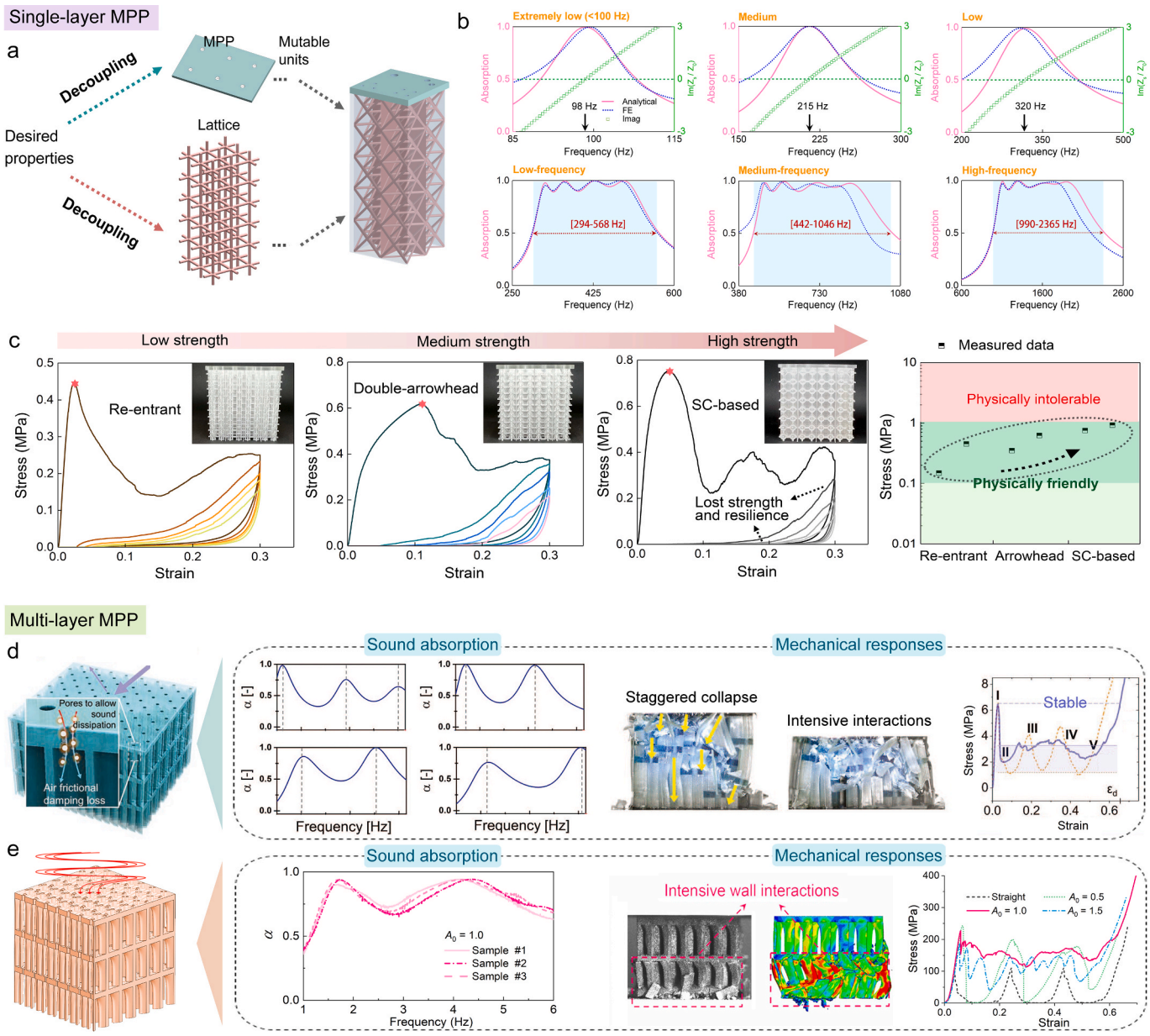

Fig. 9. Weakly coupled AMMs. (a) Schematic of a typical weakly coupled system, integrating a single-layer MPP with mechanical lattice units. (b) Tunable single-frequency and broadband absorption. (c) Independent tuning of mechanical properties through varied lattice geometries. Reprinted with permission from Ref. [48]. Two representative weakly coupled AMMs with multi-layer MPP: (d) Broadband absorption and improved mechanical resistance. Reprinted with permission from Ref. [53]. (e) Unprecedented high absorption with superior damage tolerance. Reprinted with permission from Ref. [61].

tailored for mechanical strength. By decoupling the structural responsibilities of acoustic and mechanical components, designers gain exceptional freedom to meet diverse performance targets within a single architecture.

Strongly coupled AMMs are characterized by symmetric and periodic architectures—such as trusses, shells, or plate lattices. The solid-phase topology not only determines stiffness, strength, and deformation, but also controls the spatial distribution of air domains that mediate acoustic interactions, as plotted in Fig. 10a. This relationship is further made explicit by extracting the air-phase geometry from a plate-based AMM composed of two parallel sections with different numbers of layers (Fig. 10b) [66]. The resulting air topology forms distinct pore–cavity networks that dictate resonant responses. These geometries can be mapped to equivalent acoustic circuits, enabling the analytical prediction of absorption spectra. Such hybrid resonance behavior underscores the importance of solid-geometry-controlled air domain features, such as pore diameters and cavity depth, as key determinants of acoustic performance.

To further highlight the structural interdependence, Fig. 10c presents the coupled acousto-mechanical performance of a large hollow-tube lattice [46], which exhibits broadband sound absorption attributed to the tube-resonance effect discussed before, along with damage-tolerant deformation characterized by the long stress plateaus. Fig. 10d shows a multi-sheet strategy-based AMM [55], corresponding to the design illustrated in Fig. 5b. This structure demonstrates ultra-high absorption peaks, with a pronounced absorption valley emerges around 3 ~ 4 kHz. Mechanically, it features two distinct plateau stages, indicating decent energy absorption capacity. Overall, both of these strongly coupled AMMs exhibit promising acousto-mechanical performance. But they remain unoptimized, and significant potential exists for further improvement through targeted structural refinement.

Note that while acoustic responses can often be predicted using

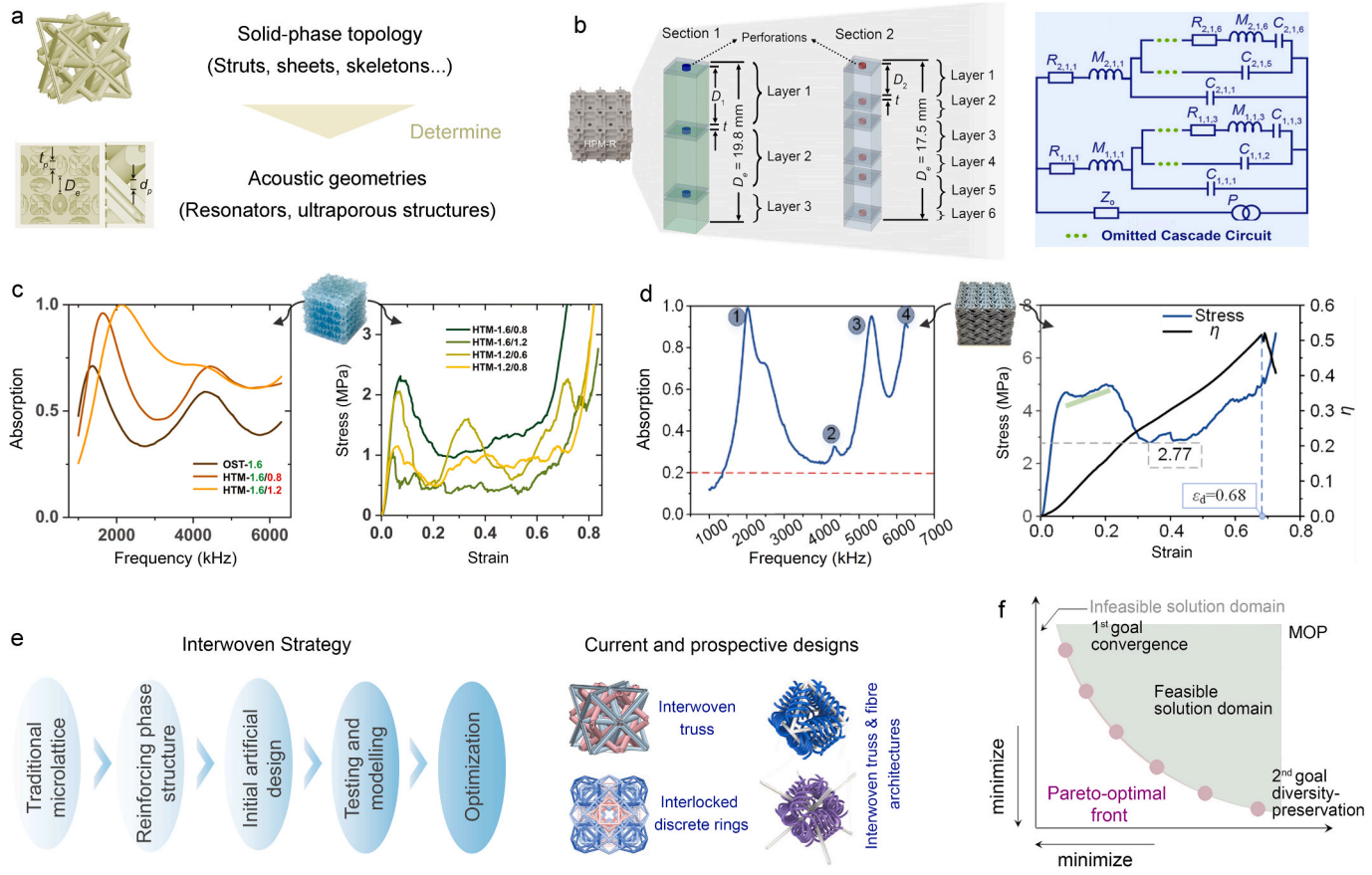

Fig. 10. Strongly coupled AMMs. (a) Solid architectures governing acoustic geometries. (b) Representative AMM with resonator-forming air domains and corresponding acoustic–electrical circuit analogy. Reprinted with permission from Ref. [66]. Experimental sound absorption and mechanical response curves for AMMs incorporating (c) tube-resonance enhancement and (d) multi-sheet designs. Reprinted with permission from Refs. [46,55]. (e) Generalized interwoven design strategy for strongly coupled systems with representative current and prospective designs displayed. Reprinted with permission from Refs. [126,127]. (f) MOP strategy yielding Pareto-optimal solutions that balance acoustic and mechanical performance. Reprinted with permission from Ref. [58].

impedance-based models, mechanical performance—particularly under nonlinear, large-strain deformation—remains analytically elusive. This inherent dichotomy creates a persistent design dilemma: geometric modifications to enhance acoustic absorption invariably degrade mechanical robustness, and vice versa. To address this tight coupling, we propose a multivariate co-optimization framework that strategically exploits synergies between antagonistic performance metrics through coordinated architectural engineering. A generalized interwoven design strategy for these systems is illustrated in Fig. 10e. Starting from a primitive lattice—whether trusses, plates, or shells—the solid framework and fluid (air) pathways are analyzed to identify a spatially complementary reinforcing phase that creates the desired resonant air domains. Analytical modeling and high-fidelity simulations then distill the key geometric parameters governing coupled acoustic–mechanical performance. A multi-objective optimization routine is applied subsequently to maximize both acoustic efficacy and mechanical robustness. The interwoven truss architecture in Fig. 10e demonstrates geometrically coherent multifunctional integration, where topological continuity ensures simultaneous mechanical-acoustic synergy. This design paradigm could be extended to other emerging interwoven architectural systems—including mechanically interlocked discrete rings [126] and textile-inspired truss-fiber hybrids [127]—which achieve unprecedented programmability in mechanical properties. Beyond load-bearing prowess, these interwoven configurations hold significant potentials for offering controllable, high-efficiency airborne sound absorption. This dual functionality positions interwoven metamaterials as prime AMM candidates. As shown in Fig. 10f, the resulting Pareto front delineates optimal trade-offs between acoustic and structural metrics. Although demonstrated in two dimensions, the framework is extendable to higher-dimensional design spaces, incorporating additional criteria such as absorption bandwidth, stiffness, energy dissipation, or fabrication constraints.

Challenges

Challenges in additive manufacturing

Despite the promising multifunctional performance of AMMs, translating intricate designs into physical structures remains a formidable challenge. This bottleneck arises primarily from limitations in additive manufacturing (AM) technologies, which impact fabrication fidelity, scalability, and reproducibility. Key issues include: (i) process-dependent variability in surface quality, dimensional accuracy, and intrinsic material properties; (ii) geometric distortions and inconsistencies between designed and fabricated architectures; and (iii) the resolution-size tradeoff, a critical constraint for fabricating sub-millimeter features and enabling practical applications.

As illustrated in Fig. 11a, even AMMs with identical geometry fabricated via different techniques such as fused filament fabrication (FFF) and stereolithography (SLA), can yield significantly different absorption spectra. This sensitivity is further highlighted in the comparative study by Tomasz et al. [72], which reported notable acoustic performance discrepancies across eight AM techniques. Microscopy tools such as optical imaging or scanning electron microscopy (SEM) are recommended to quantify geometric errors, especially in pore diameter, where deviations as small as 0.05 ~ 0.1 mm can lead to marked changes

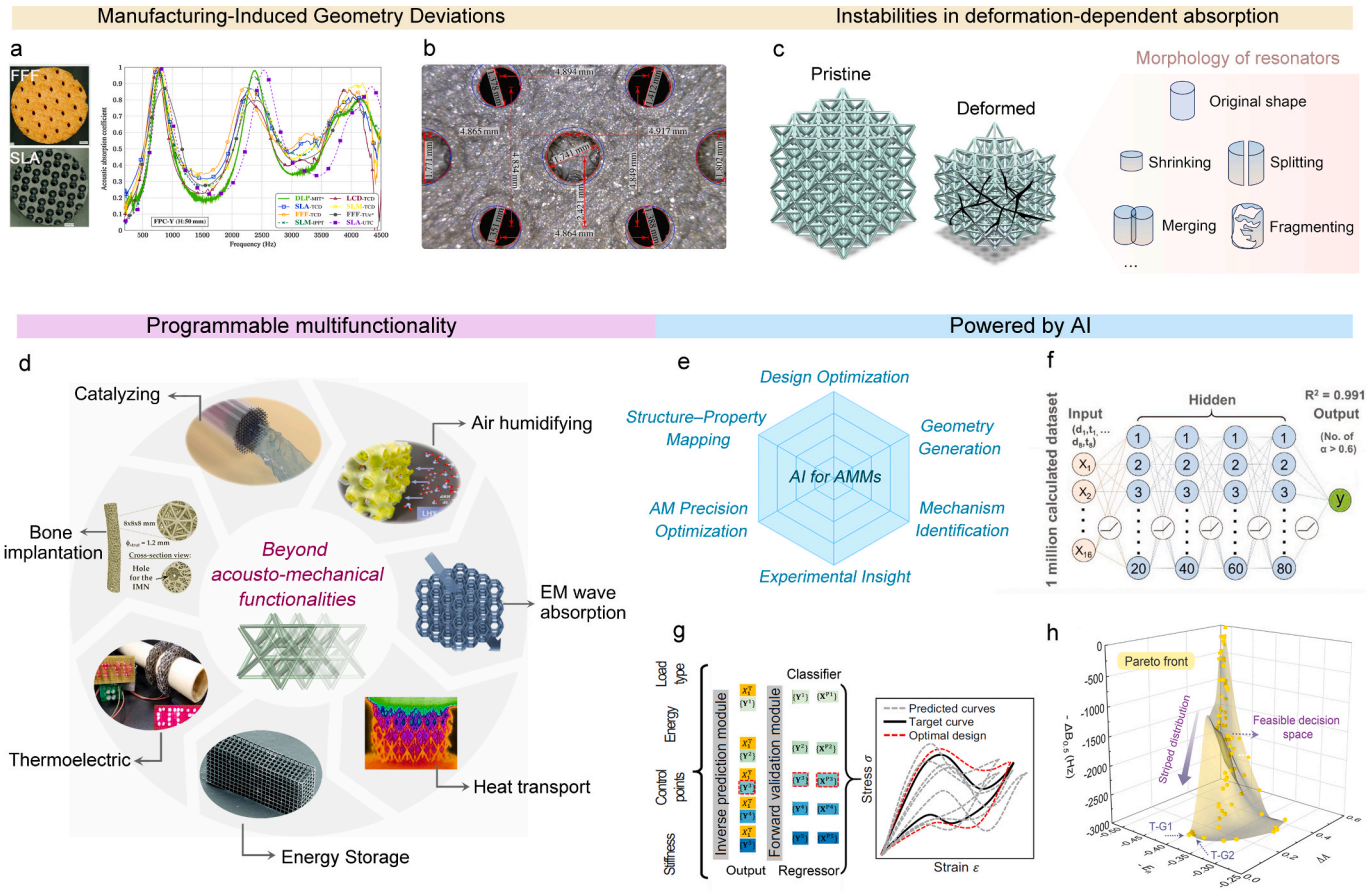

Fig. 11. Challenges and future directions for AMMs. (a) Sound absorption spectra of architected materials with identical designs but fabricated using different AM techniques. Reprinted with permission from Ref. [72]. (b) Comparison between designed (blue) and fabricated (red) pore diameters. Reprinted with permission from Ref. [128]. (c) Schematic of challenges in deformation-dependent absorption. Future directions: (d) Broadening the functional scope of architected materials beyond acousto-mechanical performance. Reprinted with permission from Refs. [133–135,141–144]. (e) The emerging role of AI in AMM design and optimization. (f) Machine learning models for predicting sound absorption bandwidths. Reprinted with permission from Ref. [89]. (g) AI-assisted prediction of mechanical responses under large strain. Reprinted with permission from Ref. [145]. (h) Multi-objective optimization for generating Pareto fronts. Reprinted with permission from Ref. [58]. (For interpretation of the references to colour in this figure legend, the reader is referred to the web version of this article.)

in acoustic behavior. In Fig. 11b, a comparison between designed (blue) and printed (red) pore sizes highlight typical dimensional mismatches [128]. As shown in Fig. 7b, smaller RVE sizes render the absorptive behavior more susceptible to printing defects. To mitigate the adverse impact of such deviations, additive manufacturing processes with the highest attainable precision should be prioritized.

Moreover, resolution is often confused with precision but constitutes a distinct challenge: it defines the minimum feature size that can be reliably fabricated within the constraints of the resolution-size tradeoff. As discussed in Section Size-dependent behaviors, reducing unit-cell size generally enhances both mechanical and acoustic properties—but this does not imply "smaller is always better." This optimization is inherently limited by the resolution-size tradeoff in additive manufacturing, where higher-resolution fabrication of microscale features (e.g., 1 μm) may demonstrate excellent performance but are rarely scalable for real-world use. Current AMM applications typically operate at the millimeter-to-centimeter scale (e.g., 1 ∼ 10 cm), aligning with structural demands in practical settings. Pushing feature sizes into the nanoscale introduces several challenges: (i) the resolution-size tradeoff dictates that smaller precision inherently leads to a reduction in the size of printed samples and untenable print times; (ii) advanced nanofabrication techniques are expensive, time-consuming, and not suited for mass production; and (iii) the acoustic gains may not sufficiently surpass those of existing porous media (e.g., foams), unless mechanical or other functional benefits are simultaneously realized. In this context, resolution should be viewed not as a target for extreme miniaturization but as a critical design constraint governed by practical scalability.

Absorptive dynamics under structural deformation

Current investigations of sound-absorptive responses in AMMs remain confined to static structural morphology, neglecting the effect of structural deformation on acoustic absorption. We introduce the concept of absorptive dynamics—a regime where mechanical compliance and sound absorption coevolve during structural deformation, fundamentally challenging conventional design paradigms. As demonstrated in Fig. 11c, resonators in their pristine state exhibit predictable absorption spectra governed by designed geometries. However, under quasi-static or dynamic loading, structural alterations—including unit-cell morphology distortion and interconnectivity change, result in non-deterministic shifts in intrinsic resonance frequencies. The resonators' geometric deviations such as shrinking, splitting, merging, and fragmenting, disrupt engineered impedance-matching conditions. Consequently, time-dependent morphological instabilities degrade both local resonance coherence and global wave interference patterns, generating erratic absorption spectrum modulation.

The observed instabilities present critical experimental challenges stemming from a fundamental disconnect: impedance tube measurements capture only static states (pristine or deformed), while transient frequency shifts during deformation evade detection. Furthermore,

microscale heterogeneities—including pore-wall roughness and residual stress gradients—induce divergent geometric outcomes under identical macroscale strains, confounding reproducibility. Theoretical frameworks face parallel constraints: Frequency-domain models inherently assume fixed boundaries, while time-domain approaches demand precise temporal resolution of deformation trajectories—requirements incompatible with complicated geometric evolution. These challenges fundamentally reshape the research paradigm in AMMs. Decoding the intricate interplay between large-strain deformation and acoustic functionalities is significant in this regime. This necessitates pioneering methodologies that leverage multi-physics coupling mechanisms, where machine intelligence could correlate strain patterns with acoustic geometries. Such methodological advancements would ultimately empower AMMs to achieve reliable performance in adaptive noise suppression systems experiencing time-varying mechanical loads, where real-time geometric reconfiguration governs operational efficacy.

Future directions

Beyond acousto-mechanical functionalities

Additive-manufactured architected acousto-mechanical materials are now emerging as a versatile platform for engineering application-driven multifunctionality [129]. This shift is underpinned by their exceptional geometric programmability and topological tunability, which allow designers to manipulate physical fields in space and scale with unprecedented precision. Unlike conventional materials, these architected systems can integrate and localize multiple functional domains—mechanical, thermal, electrical, acoustic, or even biological—within a single structural framework [129–132]. Such multifunctional integration is not merely additive; it redefines the way performance is distributed and optimized across scales. Recent studies demonstrate the potentials of extending acousto-mechanical metamaterials into domains such as electromagnetic wave absorption, catalytic reaction support, air humidity regulation, energy storage, thermoelectric conversion, and even biomedical implants.

As shown in Fig. 11d, Zhang et al. [133] developed a wood-inspired microlattice catalyst featuring overlapping bimodal pores that decouple mechanical strength, transport efficiency, and catalytic activity. With a 70 % overlap design, the structure entails a threefold increase in mechanical strength, a fourfold enhancement in normalized reaction kinetics, and a significantly enlarged surface area for catalytic functionality. Daniel et al. [134] introduced a biomimetic lichen–Schwarz metamaterial, which combines TPMS-based lattice architecture with natural lichen. It achieves both selective sound blocking and humidity regulation, exemplifying the potentials of developing eco-functional materials not only but noise reduction. By using the unique parent material, architected materials also serve as electromagnetic wave absorbers [135], making them highly relevant for defense and communication applications. When combined with acoustic absorption, they provide a dual-mode energy dissipation system for extreme environments. Critically, elastic metamaterials exemplify a paradigm where structural rigidity and elastic wave manipulation coexist—a cornerstone for advancing multifunctional AMMs. These systems leverage high-stiffness architectures to ensure structural integrity, while offering reconfigurable design capabilities for tailoring elastic wave propagation—primarily through dispersion engineering strategies at the structural level [136–138]. This capability can be further harnessed in the acousto-mechanical platform, where dispersion-tailored AMMs simultaneously suppress structural vibrations and mitigate radiated noise. Such an approach offers a unified strategy for broadband wavefront shaping across hybrid wave domains [139,140]. By harmonizing these principles, AMMs evolve into unified platforms capable of synergizing mechanical performance with dynamic wave manipulation. Besides, leveraging the porous characteristics, the thermal transport in microlattices can be engineered for developing thermo-insulative or thermomechanical metamaterials [141]. With superior mechanical properties, lattice architecture could be programmed for varying directional stiffness for bone implant application [142], thermoelectric generators [143], and employed as lightweight electrodes for exceptional electrochemical performance [144].

The shift from function-specific to multifunctional architected materials marks a transformative paradigm in material systems engineering—one in which geometry, hierarchy, and composition are elevated from passive design elements to active, tunable variables. Crucially, in the context of AMMs, this evolution does not imply abandoning their core acoustic and structural capabilities. Rather, it highlights their potential as foundational frameworks for integrating additional functionalities without compromising their original performance. Through structure control, AMMs serve as a convergent platform for embedding diverse physical behaviors—including thermal regulation, electromagnetic attenuation, fluid transport, or catalytic activity—within a unified structure. This “all-in-one” functionality is made feasible by the inherent decoupling and reconfigurability afforded by additive manufacturing, enabling different domains to coexist and interact synergistically. Looking ahead, AMMs are uniquely positioned to deliver integrated solutions that address the complex demands of next-generation technologies—not by replacing one function with another, but by uniting them within a single, programmable architecture.

AI-driven development

Artificial intelligence (AI) is increasingly becoming a transformative force in the development of AMMs. As discussed in previous sections, computational methodologies have demonstrated strong potential for accelerating performance-driven design. AI enables both targeted single-property optimization—such as maximizing absorption in weakly coupled systems—and multi-objective balancing, where acoustic and mechanical demands must be simultaneously satisfied.

As illustrated in Fig. 11e, AI contributes to AMMs development through six tightly integrated functional directions. These include: (i) rapid design optimization via machine learning-assisted inverse design tools, (ii) generative topology creation using data-driven algorithms to produce acoustically and mechanically efficient architectures, (iii) structure–property mapping that builds predictive models linking geometric descriptors (e.g., pore diameter, ligament connectivity, shell thickness) to functional outputs such as stiffness or absorption, (iv) additive manufacturing precision optimization by detecting and correcting deviations that affect pore fidelity and local wall geometry, (v) mechanism discovery and refinement through physics-informed learning to understand resonance modes, impedance profiles, and loss mechanisms, and (vi) data-driven insight extraction from experimental datasets, enabling researchers to uncover correlations, anomalies, or failure patterns that may be imperceptible through manual analysis. Together, these six capabilities establish a comprehensive framework where AI not only accelerates design and fabrication but also expands the fundamental understanding of acousto-mechanical performance.

Fig. 11f presents an example where ANN is applied to optimize perforation parameters in MPP-based lattice absorbers [89]. Out of a design space with over 79 million combinations, one million configurations were simulated to form a training dataset, with 16 input parameters and output labels defined as the number of frequency points where the absorption coefficient α exceeds 0.6. The trained model enables rapid prediction of high-performance MPP configurations, greatly accelerating the exploration process. Another use case of AI is shown in Fig. 11g, which presents a generative machine learning pipeline for predicting full stress–strain curves [145]. This framework consists of an inverse prediction module and a forward validation module, incorporating a curve-type classifier and a curve-feature regressor. By learning from a curated dataset, the system can generate tailored stress–strain responses based on target performance requirements, enabling AI-guided mechanical optimization. Fig. 11h highlights how MOP is

employed to simultaneously tune elastic stiffness, isotropy, and acoustic bandwidth [58]. The resulting Pareto front—visualized in a 3D design space—identifies feasible decision zones that meet multiple conflicting criteria, providing a rational basis for trade-off navigation in strongly coupled AMM systems.

Collectively, these examples highlight AI's revolutionary role in advancing AMMs—not simply as an optimization tool, but as a catalyst for intelligent, adaptive material systems. As AMMs continue to grow in structural complexity and multifunctional demands, the integration of AI will be essential to navigate vast design spaces, decode hidden structure–function correlations, and bridge simulation with real-world fabrication constraints. This synergy between AI and architected materials holds immense promise for realizing high-performance, adaptive, and application-specific metamaterials that were previously unattainable through traditional means. Looking forward, the fusion of AI with advanced physics-based modeling and high-fidelity manufacturing is poised to redefine not only how AMMs are designed, but also how they evolve—intelligently and autonomously—toward their next frontier of functionality.

Applications and broader impact

AMMs offer a unified platform to simultaneously control sound energy and manage structural loads. By leveraging architected topologies, AMMs enable decoupling or integration of mechanical and wave-based responses—unlocking multifunctionality across diverse engineering sectors [4,146]. As shown in Table 2, in the transportation sector, AMMs address key challenges in next-generation mobility systems. Applications in EVs (electric vehicles), high-speed trains, and low-altitude aircraft such as UAVs (unmanned aerial vehicle) and eVTOLs (electric vertical take-off and landing aircraft) demand lightweight materials that absorb cabin noise, mitigate vibration, and absorb crash energy. For instance, in high-speed trains, the central challenge lies in reconciling structural integrity with broadband noise attenuation across low-to-high frequencies. AMM-integrated interior panels (sidewalls, flooring, ceilings) effectively attenuate cabin noise originating from wheel-rail interactions and aerodynamic sources, while fulfilling stringent mechanical requirements: static strength for vehicle integrity and impact resistance against high-velocity debris. Similarly, in aerospace and defense, AMMs enable both acoustic stealth and strong load-bearing components—nacelle liners, missile casings, and drone fuselages. These systems leverage tuned impedance to noises while enhancing thermal–mechanical resilience. For example, in aircraft engines, mechanically robust AMM liners—strategically integrated within inlet or bypass duct sections—dissipate low-frequency combustion noise through tuned cavity resonances, while withstanding high-pressure airflow. Engine-mounted acoustic liners exemplify this dual functionality, featuring aerodynamic conformal designs that maintain operational efficiency under extreme thermal cycling. For industrial equipment, such as compressor enclosures, data centers, and substations, AMMs enable noise suppression under thermomechanical stress. These environments require durable materials that withstand thermal cycling, mechanical vibration, and acoustic loading. AMMs—especially those with tuned porosity—can be engineered to attenuate frequency-specific noise while simultaneously serving as load-bearing supports or thermal dissipators. In architectural acoustics, AMMs can be deployed in tunnels, modular wall panels, theaters, and smart interiors. Compared to conventional absorbers, AMMs offer higher design flexibility and integration potential. Their load-bearing capability allows for multifunctional walls and ceilings that combine structural rigidity, broadband sound control, and even aesthetic surface modulation. Modular AMM units could adapt dynamically to changing acoustic environments, particularly when combined with sensor-actuator networks or AI-assisted control systems.

It is worthy to note that, while this review focus on the field of airborne sound absorption and mechanical functionality, the definition of "acousto-mechanical" coupling is not confined to these domains. Emerging frontiers—particularly at micro-/bio-interfaces—reveal expanded operational modalities: acoustic-to-mechanical energy conversion in tympanic membranes, ultrasound-induced hemodynamic modulation, and acousto-mechanical signal transduction in biological tissues [147,148]. At the micro-electromechanical-systems (MEMS) scale, acousto-mechanical coupling can be engineered into tunable architectures for enhanced energy harvesting by manipulating wave propagation (e.g., focusing and localization) and amplifying strain in energy conversion materials [149]. Recent advances in MEMS-based tunable metamaterials leverage electrothermal, electrostatic, and electromagnetic actuators to dynamically reconfigure unit cells, enabling precise control of electromagnetic wave properties (amplitude, frequency, phase, polarization) [150]. Such cross-domain programmability could be exemplified in biointegrated systems. A notable example from Rogers et al. [151] demonstrates a microscale wireless platform that uses acoustic signatures to non-invasively interrogate internal tissue mechanics, enabling continuous health monitoring and wearable technologies.

Beyond biomedical domains, AMMs present a structurally programmable route toward advanced wave-based functionalities—including vibro-acoustic cloaking, embedded waveguides, tunable resonators, and nonlinear impedance-matched interfaces for sensors and transducers. These applications require strong geometry-governed coupling and precise spatial control—capabilities inherently supported by architected lattices. Viewed more broadly, AMMs represent not merely a class of materials, but a design paradigm where structure, function, and information are intrinsically linked. As fabrication and design tools continue to advance, AMMs are poised to enable programmable responses across domains—paving the way for intelligent and adaptive multifunctional systems.

Summary

This review crystallizes critical insights into the structural design strategies and physical principles that empower acousto-mechanical metamaterials (AMMs)—a rapidly emerging class of architected materials—to deliver unprecedented airborne sound absorption and mechanical properties. While AMMs inherently benefit from the mechanical efficiency of architectural topologies, the key design challenge lies in enabling effective and broadband sound absorption within compact geometries. We introduce a unified design framework that classifies AMMs into primitive, additive, and subtractive topologies, and analyze how these configurations govern resonant behavior and dissipative mechanisms. We further propose three key enhancement

Table 2
Representative engineering applications of AMMs.

Application Domain	Transportation	Aerospace & Defense	Industrial Equipment	Architectural Acoustics	Emerging Technologies
Representative Scenarios	EV interiors, high-speed trains, UAVs, eVTOLs	Aircraft cabins, engine nacelle liners, missiles, drones	Substations, compressor halls, data centers, turbines	Tunnels, theaters, smart walls, modular construction panels	Metamaterials, vibro-acoustic cloaking, ultrasonic devices
Functional Requirements	Lightweight property, noise absorption, impact energy absorption	Acoustic stealth, thermal/vibration control, impact mitigation	Noise absorption, load-bearing, structural damping, thermal resilience	Sound attenuation, modular acoustic panels, structural support	Wave control, acoustic filtering, vibration isolation

strategies—coherently coupled weak resonators, structural geometry optimization, and lossy-layer integration—which together provide physics-informed routes to overcome absorption dips and approach the causality-governed efficiency–thickness limit. Furthermore, a critical contribution of this review is the elucidation of acousto-mechanical coupling mechanisms. By examining the influence of parent material stiffness, unit-cell scale, and geometric interdependence, we reveal how shared or separable architecture governs the correlation between acoustic and mechanical functionalities. A three-tier coupling classification—weak, moderate, and strong—offers a predictive framework to assess whether these properties can be independently tuned or must be co-optimized under inherent trade-offs. Finally, we discuss the challenges of achieving precise additive manufacturing and maintaining stable sound absorption under large-strain deformation, and highlight future directions in AI-guided development, multifunctionality, and real-world deployment. Positioned at the intersection of geometry, material science, and physical modeling, AMMs are not merely dual-function structures—but a versatile design platform for programmable, multifunctional systems across engineering domains.

CRediT authorship contribution statement

Zhendong Li: Writing – review & editing, Writing – original draft, Data curation, Conceptualization. **Xinxin Wang:** Writing – review & editing. **Zhonggang Wang:** Resources, Investigation, Funding acquisition. **Xinwei Li:** Writing – review & editing, Methodology. **Xiang Yu:** Writing – review & editing, Investigation. **Seeram Ramakrishna:** Supervision, Investigation. **Yang Lu:** Writing – review & editing, Methodology, Conceptualization. **Li Cheng:** Writing – review & editing, Methodology, Funding acquisition, Formal analysis, Conceptualization.

Declaration of competing interest

The authors declare that they have no known competing financial interests or personal relationships that could have appeared to influence the work reported in this paper.

Acknowledgments

The authors acknowledge the support from NSFC/RGC Joint Research Scheme sponsored by the Research Grants Council of Hong Kong and the National Natural Science Foundation of China (N_PolyU553/23), RGC Theme-based Research Scheme (P0053908 under parent project P0047801), Hunan Provincial Natural Science Foundation of China (2023JJ10074), and the Science and Technology Innovation Program of Hunan Province (2023RC1011).

Data availability

No data was used for the research described in the article.

References

[1] Murphy, E., and King, E. A., Environmental noise pollution: Noise mapping, public health, and policy. Elsevier: 2022.
[2] M. Basner, et al., Lancet 383 (9925) (2014) 1325.
[3] H. Brumm, et al., Sci. Adv. 7 (20) (2021) eabe2405.
[4] S. Huang, et al., Phys. Rev. Appl 20 (1) (2023) 010501.
[5] Y.I. Bobrovnitskii, T. Tomilina, Acoust. Phys. 64 (2018) 519.
[6] S.A. Cummer, et al., Nat. Rev. Mater. 1 (3) (2016) 1.
[7] E. Dong, et al., Natl. Sci. Rev. 10 (6) (2023) nwac246.
[8] N. Gao, et al., Adv. Mater. Technol. 7 (6) (2022) 2100698.
[9] Y. Li, B.M. Assouar, Appl. Phys. Lett. 108 (6) (2016) 063502.
[10] Y. Zhu, et al., Phys. Rev. B 103 (6) (2021) 064102.
[11] K. Donda, et al., Appl. Phys. Lett. 115 (17) (2019) 173506.
[12] H. Long, et al., Appl. Phys. Lett. 111 (14) (2017) 143502.
[13] H.-W. Dong, et al., Mater. Today (2024).
[14] S.H. Mousavi, et al., Nat. Commun. 6 (1) (2015) 8682.
[15] M.-H. Lu, et al., Mater. Today 12 (12) (2009) 34.
[16] Y. Si, et al., Nat. Commun. 5 (1) (2014) 5802.
[17] Y. Si, et al., Sci. Adv. 4 (4) (2018) eaas8925.
[18] Y. Zhao, et al., ACS Nano 17 (16) (2023) 15615.
[19] J. Fan, et al., Int. J. Mech. Sci. 238 (2023) 107848.
[20] Y. Liu, et al., J. Mech. Phys. Solids 190 (2024) 105751.
[21] D.W. Wang, et al., Mater. Des. 186 (2019) 108344.
[22] Y. Tang, et al., Compos. Struct. 226 (OCT.), 1 (2019).
[23] Y. Tang, et al., Sci. Rep. 7 (1) (2017) 43340.
[24] W. Zhang, F. Xin, J. Sound Vib. 578 (2024) 118330.
[25] M.G. Jones, et al., AIAA J. 60 (4) (2022) 2481.
[26] T.A. Schaedler, et al., Science 334 (6058) (2011) 962.
[27] X. Zheng, et al., Science 344 (6190) (2014) 1373.
[28] W.W.S. Ma, et al., Adv. Sci. (2025) 2405835.
[29] T. Maconachie, et al., Mater. Des. 183 (2019) 108137.
[30] Y. Wang, et al., Sci. Adv. 10 (35) (2024) eadq2664.
[31] T. Yang, et al., Proc. Natl. Acad. Sci. 117 (38) (2020) 23450.
[32] T. Yang, et al., Science 375 (6581) (2022) 647.
[33] L.R. Meza, et al., Science 345 (6202) (2014) 1322.
[34] L.R. Meza, et al., Proc. Natl. Acad. Sci. 112 (37) (2015) 11502.
[35] X. Zhou, et al., Compos. Struct. 354 (2025) 118794.
[36] Z. Xiao, et al., Mater. Des. 241 (2024) 112912.
[37] X. Li, et al., Adv. Mater. Technol. (2025) 2500118.
[38] Y. Tang, et al., Mater. Des. 134 (2017) 502.
[39] J. Liu, et al., Constr. Build. Mater. 472 (2025) 140852.
[40] X. Zhang, et al., AIP Adv. 6 (2016) 10.
[41] L. Li, et al., Mater. Des. 241 (2024) 112946.
[42] M. Zhao, et al., Int. J. Minerals Metallurgy Mater. 30 (10) (2023) 1973.
[43] L. Li, et al., Int. J. Mech. Sci. 269 (2024) 109071.
[44] Y. Huang, et al., Thin-Walled Struct. 199 (2024) 111815.
[45] J. Feng, et al., Small 20 (42) (2024) 2403254.
[46] X. Li, et al., Small 18 (44) (2022) 2204145.
[47] X. Li, et al., Small 17 (24) (2021) 2100336.
[48] Z. Li, et al., Mater. Horiz. 10 (1) (2023) 75.
[49] C. Yu, et al., Adv. Sci. 11 (22) (2024) 2400250.
[50] Z. Yu, et al., Compos. Sci. Technol. 256 (2024) 110765.
[51] J. Feng, et al., Int. J. Mech. Sci. 287 (2025) 109920.
[52] X. Li, et al., Adv. Sci. 11 (4) (2024) 2305232.
[53] X. Li, et al., Adv. Funct. Mater. 33 (2) (2023) 2210160.
[54] H. Wang, et al., Adv. Eng. Mater. 26 (23) (2024) 2401686.
[55] J. Zhang, et al., Compos. Struct. 325 (2023) 117589.
[56] J.W. Chua, et al., Compos. Struct. 304 (2023) 116434.
[57] Z. Li, et al., ACS Appl. Mater. Interfaces 15 (7) (2023) 9940.
[58] Z. Li, et al., Adv. Funct. Mater. (2024) 2420207.
[59] Z. Lai, et al., Materials Science in Additive Manufacturing 1 (4) (2022) 22.
[60] W. Yang, et al., Virtual and Physical Prototyping 15 (2) (2020) 242.
[61] Z. Li, et al., NPG Asia Mater. 16 (1) (2024) 45.
[62] X. Li, et al., Adv. Mater. Technol. 10 (4) (2025) 2400517.
[63] M. Yang, et al., Mater. Horiz. 4 (4) (2017) 673.
[64] Z. Zhou, et al., Natl. Sci. Rev. 9 (8) (2022) nwab171.
[65] V. Sekar, et al., Virtual and Physical Prototyping 19 (1) (2024) e2435562.
[66] Z. Li, et al., Virtual and Physical Prototyping (2022).
[67] L. Huang, et al., Nat. Rev. Phys. 6 (1) (2024) 11.
[68] G. Ma, et al., Nat. Mater. 13 (9) (2014) 873.
[69] C. Zhang, X. Hu, Phys. Rev. Appl 6 (6) (2016) 064025.
[70] O.R. Bilal, et al., Phys. Rev. Appl 10 (2018) 5.
[71] X. Zhang, et al., Appl. Acoust. 151 (2019) 22.
[72] T.G. Zieliński, et al., Addit. Manuf. 36 (2020) 101564.
[73] Z. Wang, et al., Virtual and Physical Prototyping 18 (1) (2023) e2111585.
[74] M. Zhao, et al., Compos. Struct. 295 (2022) 115830.
[75] M. Zhao, et al., Int. J. Mech. Sci. 238 (2023) 107842.
[76] Y. Liu, et al., Nat. Commun. 15 (1) (2024) 2984.
[77] Z. Li, et al., ACS Appl. Mater. Interfaces 15 (20) (2023) 24868.
[78] N. Jiménez, et al., Appl. Phys. Lett. 109 (2016) 12.
[79] N. Jiménez, et al., Sci. Rep. 7 (1) (2017) 13595.
[80] G. Serra, et al., Mech. Syst. Sig. Process. 202 (2023) 110707.
[81] Y. Wang, et al., Small 19 (18) (2023) 2206024.
[82] C. Crook, et al., Nat. Commun. 11 (1) (2020) 1579.
[83] T. Tancogne-Dejean, et al., Adv. Mater. 30 (45) (2018) 1803334.
[84] J.U. Surjadi, C.M. Portela, Nat. Mater. (2025) 1.
[85] B. Wojciechowski, et al., Addit. Manuf. 71 (2023) 103608.
[86] Z. Li, et al., Virtual and Physical Prototyping 18 (1) (2023) e2166851.
[87] Maa, D.-Y., *the Journal of the Acoustical Society of America* (1998) **104** (5), 2861.
[88] U. Ingard, J. Acoust. Soc. Am. 26 (2) (1954) 151.
[89] X. Li, et al., Adv. Mater. 33 (44) (2021) 2104552.
[90] M.-T. Hsieh, et al., J. Mech. Phys. Solids 125 (2019) 401.
[91] A. Guell Izard, et al., Small 15 (45) (2019) 1903834.
[92] J. Allard, N. Atalla, *Propagation of sound in porous media: modelling sound absorbing materials*, John Wiley & Sons, 2009.
[93] M.R. Stinson, J. Acoust. Soc. Am. 89 (2) (1991) 550.
[94] X. Li, et al., Mater. Horiz. 10 (8) (2023) 2892.
[95] K. Wang, et al., Device 2 (2024) 10.
[96] A.D. Pierce, *Acoustics: an introduction to its physical principles and applications*, Springer, 2019.
[97] H. Ding, et al., Int. J. Mech. Sci. 232 (2022) 107601.
[98] S. Fan, et al., J. Opt. Soc. Am. A 20 (3) (2003) 569.
[99] S. Huang, et al., Science Bulletin 65 (5) (2020) 373.
[100] C. Shao, et al., Appl. Phys. Lett. 120 (2022) 8.

[101] Z. Wang, et al., Appl. Phys. Lett. 119 (2021) 17.
[102] V. Romero-García, et al., Sci. Rep. 6 (1) (2016) 19519.
[103] Y.-X. Gao, et al., Sci. Rep. 10 (1) (2020) 10705.
[104] F. Wu, et al., Appl. Phys. Lett. 114 (2019) 15.
[105] G.d.N. Almeida, et al., Appl. Acoust. 172 (2021) 107593.
[106] M. Yang, et al., Comptes Rendus Mécanique 343 (12) (2015) 635.
[107] Y.S. Choy, et al., Compos. B Eng. 40 (4) (2009) 259.
[108] S. Yu, et al., Adv. Funct. Mater. 34 (14) (2024) 2312835.
[109] A. Treviso, et al., Compos. B Eng. 78 (2015) 144.
[110] L. Cao, et al., Compos. Commun. 10 (2018) 25.
[111] S. Koch, et al., J. Sound Vib. 393 (2017) 30.
[112] F. Ma, et al., Mater. Horiz. 9 (2) (2022) 653.
[113] S. Cui, R.L. Harne, Phys. Rev. Appl 12 (6) (2019) 064059.
[114] E.C. Clough, et al., Matter 1 (6) (2019) 1519.
[115] Z.P. Bažant, Int. J. Solids Struct. 37 (1–2) (2000) 69.
[116] N. Hansen, Scr. Mater. 51 (8) (2004) 801.
[117] M. Yoder, et al., Int. J. Solids Struct. 143 (2018) 245.
[118] W. Zhang, et al., International Journal of Extreme Manufacturing 4 (4) (2022) 045201.
[119] J. Bauer, et al., Adv. Mater. 29 (40) (2017) 1701850.
[120] J. Costa-Baptista, et al., Addit. Manuf. 55 (2022) 102777.
[121] Z. Hu, et al., Virtual and Physical Prototyping 19 (1) (2024) e2412198.
[122] J. Fan, et al., Mater. Today 50 (2021) 303.
[123] W. Chen, et al., Sci. Adv. 5 (9) (2019) eaaw1937.
[124] J. Berger, et al., Nature 543 (7646) (2017) 533.
[125] T. Tancogne-Dejean, et al., Acta Mater. 116 (2016) 14.
[126] W. Zhou, et al., Science 387 (6731) (2025) 269.
[127] J.U. Surjadi, et al., Nat. Mater. (2025) 1.
[128] K.C. Opiela, T.G. Zieliński, Compos. B Eng. 187 (2020) 107833.
[129] P. Jiao, et al., Nat. Commun. 14 (1) (2023) 6004.
[130] Z. Zhang, et al., Compos. Sci. Technol. 216 (2021) 109064.
[131] K.J. Maloney, et al., Int. J. Heat Mass Transf. 55 (9–10) (2012) 2486.
[132] X. Li, et al., Mater. Des. 234 (2023) 112354.
[133] L. Zhang, et al., Nat. Commun. 15 (1) (2024) 2046.
[134] D. Saatchi, et al., Adv. Funct. Mater. 33 (31) (2023) 2214580.
[135] J. Lee, et al., Small 19 (50) (2023) 2305005.
[136] G. Lee, et al., Adv. Sci. 11 (19) (2024) 2400090.
[137] S.-M. Yuan, et al., Mech. Syst. Sig. Process. 179 (2022) 109371.
[138] J. Park, et al., Adv. Funct. Mater. 35 (2) (2025) 2412901.
[139] G. Lee, et al., Proc. Natl. Acad. Sci. 122 (18) (2025) e2425407122.
[140] H.-W. Dong, et al., Natl. Sci. Rev. 9 (12) (2022) nwac030.
[141] S. Farzinazar, et al., APL Mater. 7 (2019) 10.
[142] A. Benady, et al., Mater. Des. 226 (2023) 111605.
[143] V. Karthikeyan, et al., Nat. Commun. 14 (1) (2023) 2069.
[144] K. Narita, et al., Adv. Energy Mater. 11 (5) (2021) 2002637.
[145] C.S. Ha, et al., Nat. Commun. 14 (1) (2023) 5765.
[146] M. Yang, P. Sheng, Appl. Phys. Lett. 122 (2023) 26.
[147] P. Augustsson, et al., Nat. Commun. 7 (1) (2016) 11556.
[148] Y.-J. Ho, et al., J. Control. Release 356 (2023) 481.
[149] G. Lee, et al., Mater. Today Energy 37 (2023) 101387.
[150] R.-J. Xu, Y.-S. Lin, Electronics 11 (2) (2022) 243.
[151] J.-Y. Yoo, et al., Nat. Med. 29 (12) (2023) 3137.